Contrib Mineral Petrol (1985) 91:105–121

Contributions to Mineralogy and Petrology

The speciation of carbon dioxide in sodium aluminosilicate glasses

Gerald Fine and Edward Stolper
Division of Geological and Planetary Sciences, California Institute of Technology, Pasadena, California 91125

Abstract. Infrared spectroscopy has been used to study the speciation of CO_2 in glasses near the $NaAlO_2$–SiO_2 join quenched from melts held at high temperatures and pressures. Absorption bands resulting from the antisymmetric stretches of both molecular CO_2 (2,352 cm^{-1}) and CO_3^{2-} (1,610 cm^{-1} and 1,375 cm^{-1}) are observed in these glasses. The latter are attributed to distorted Na-carbonate ionic-complexes. Molar absorptivities of 945 liters/mole-cm for the molecular CO_2 band, 200 liters/mole-cm for the 1,610 cm^{-1} band, and 235 liters/mole-cm for the 1,375 cm^{-1} band have been determined. These molar absorptivities allow the quantitative determination of species concentrations in the glasses with a precision on the order of several percent of the amount present. The accuracy of the method is estimated to be ±15–20% at present.

The ratio of molecular CO_2 to CO_3^{2-} in sodium aluminosilicate glasses varies little for each silicate composition over the range of total dissolved CO_2 content (0–2%), pressure (15–33 kbar) and temperature (1,400–1,560° C) that we have studied. This ratio is, however, a strong function of silicate composition, increasing both with decreasing Na_2O content along the $NaAlO_2$-SiO_2 join and with decreasing Na_2O content in peraluminous compositions off the join.

Infrared spectroscopic measurements of species concentrations in glasses provide insights into the molecular level processes accompanying CO_2 solution in melts and can be used to test and constrain thermodynamic models of CO_2-bearing melts. CO_2 speciation in silicate melts can be modelled by equilibria between molecular CO_2, CO_3^{2-}, and oxygen species in the melts. Consideration of the thermodynamics of such equilibria can account for the observed linear relationship between molecular CO_2 and carbonate concentrations in glasses, the proposed linear relationship between total dissolved CO_2 content and the activity of CO_2 in melts, and observed variations in CO_2 solubility in melts.

Introduction

Stimulated by the important role played by carbon dioxide in the petrogenesis of a wide range of igneous rocks, particularly alkaline basic magmas (e.g. Eggler 1973; Wyllie 1979), there has been considerable recent interest in the solubility mechanisms of CO_2 in silicate melts. Two contrasting approaches to understanding these solution mechanisms have been pursued. The first is an indirect approach that uses systematic variations in solid-liquid phase equilibria to infer structural changes that occur in melts when they dissolve CO_2. For example, the liquidus volume of pyroxene, a polymerized phase, enlarges relative to that of olivine, an unpolymerized phase, when CO_2 is added to melts. This has been used to infer that addition of CO_2 results in increased polymerization of melts (Eggler 1974, 1978; Kushiro 1975). Unfortunately, this intuitively satisfying line of reasoning has given, at best, only qualitative insights.

The second approach used to understand CO_2 solution mechanisms involves spectroscopic techniques. Both infrared (Mysen et al. 1975; Brey and Green 1975, 1976; Mysen 1976; Brey 1976; Mysen et al. 1976; Eggler et al. 1979) and Raman (Verweij et al. 1977; Sharma 1979; Sharma et al. 1979a; Mysen and Virgo 1980a, b; Rai et al. 1983) spectroscopy have been used to study CO_2-bearing silicate glasses quenched from melts to elucidate aspects of the speciation of CO_2-bearing melts. These spectroscopic techniques can provide direct, quantitative information on how, at a molecular level, carbon dioxide is dissolved in silicate glasses and how it influences the structure of the silicate framework. In particular, infrared and Raman spectroscopy can be used to distinguish between carbon dioxide that is dissolved as carbonate (CO_3^{2-}) ions and that which is dissolved as molecules of CO_2.

Most recent spectroscopic investigations have not taken full advantage of the quantitative potential of infrared or Raman spectroscopy. Most investigators have simply noted the existence of absorption or emission bands and thus of particular species in the glasses; the intensities of the bands have not generally been used to determine the concentrations of the absorbing or emitting species. Exceptions include the work of Verweij et al. (1977) in which the potential for using Raman spectroscopy to determine the concentrations of CO_3^{2-} groups in K_2O-SiO_2-CO_2 glasses was discussed and the work of Sharma and co-workers in which Raman spectroscopy was used to determine relative concentrations of CO_3^{2-} ions as a function of pressure and temperature in glasses of sodium melilite, diopside, and akermanite composition (Sharma 1979; Sharma et al 1979a). In addition, Mysen (1976) used infrared spectroscopy to estimate CO_3^{2-} concentrations in glasses on the $NaAlO_2$-SiO_2-CO_2 join. In that study, Mysen concluded that the relative proportions of molecular CO_2 groups and carbonate groups

Offprint requests to: E. Stolper

in CO_2-bearing glasses are strong functions of silicate composition and of the pressures and temperatures from which melts are quenched to glasses.

In this paper we report the results of experiments designed to more fully develop the potential of infrared spectroscopy for quantitative determinations of the concentrations of carbon-bearing species in silicate glasses. We first determine molar absorptivities (or extinction coefficients) for absorption bands due to molecular CO_2 and carbonate in glasses near the $NaAlO_2$-SiO_2-CO_2 join. Using these molar absorptivities to measure the concentrations of molecular CO_2 and carbonate in glasses, we have investigated the dependence of the speciation of CO_2 in sodium aluminosilicate glasses on glass composition, on total dissolved CO_2 content, and on the pressure and temperature of equilibration of the melt from which the glass was quenched. The results provide insights into the solubility mechanisms of CO_2 in silicate melts, into the thermodynamics of CO_2-bearing silicate melts, and into the effects of dissolved CO_2 on the phase equilibria of silicate melts.

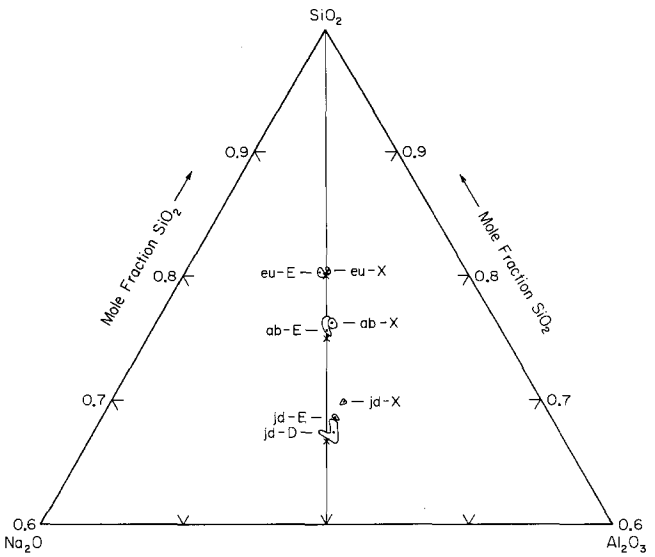

Fig. 1. Graphical representation of the starting compositions used. Ideal stoichiometric compositions are marked by X. The fields show the range of microprobe analyses, while the solid circles show the average of all analyses for each sample

Experimental techniques

Powdered silicate starting materials were prepared at three compositions along the $NaAlO_2$-SiO_2 join: $NaAlSi_2O_6$ (*jd*), $NaAlSi_3O_8$ (*ab*) and $NaAlSi_4O_{10}$ (a composition close to the 1 atm albite-silica eutectic designated as *eu*). Glasses of *jd* composition (batches *jd-D* and *jd-E*) were synthesized by grinding Na_2CO_3, Al_2O_3 and SiO_2 (Johnson-Matthey SpecPure reagents) in agate under ethanol for 6 h followed by melting at 1580° C for 12 h in air at 1 atm. Appropriate amounts of SiO_2 glass were then added to *jd-E* to prepare batches *ab-E* and *eu-E*. These decarbonated mixtures were ground under ethanol for 6 h and dried at 850° C in air at 1 atm for 2 days to remove any hydrocarbon residue or adsorbed CO_2. When mixtures not dried in this fashion were used as starting materials for our high pressure experiments, CO_2 was detected spectroscopically in the run products even when no CO_2 was loaded into the charges. Drying times of more than 1 week resulted in significant Na-loss. Some Na-depleted compositions were used as starting materials; these are designated *jd-X, ab-X,* and *eu-X*. All starting materials were stored over dessicant after drying.

Selected glasses of each composition were analyzed for major elements in order to verify glass homogeneity and to determine the extent of Na-loss during the drying process. Analyses were obtained using an automated MAC-5 electron microprobe with a 15 KV operating voltage, a sample current of 5 nA on brass and a 40–45 micron spot size (Table 1). The results of these analyses are shown graphically in Fig. 1.

The starting materials were loaded along with known amounts of silver oxalate ($Ag_2C_2O_4$) into Pt capsules, which were then sealed by arc-welding. These Pt capsules were loaded into larger Pt capsules containing a dry hematite-magnetite buffer. The amounts of silver oxalate and silicate were weighed on a Cahn electrobalance to 0.0005 mg precision out of 0.0750–20.0000 mg total and were chosen to produce vapor-undersaturated melts. The silver oxalate was analyzed by gas manometry in the laboratory of Professor S. Epstein and found to be stoichiometric to within 5% of its nominal total CO_2 content. It was stored in a light-proof container over dessicant to minimize decomposition and H_2O adsorption.

The double capsules were held at constant pressure (15–33 kbar) and temperature (1,400–1,560° C) in a 0.5 inch solid media piston-cylinder apparatus using a NaCl and pyrex cell. A hot piston-in technique was used: runs were brought cold to a pressure 5 kbar below the desired pressure, the temperature was raised to the final temperature and the final pressure was applied. Temperature was monitored using W3%Re–W25%Re thermocouples. Pressure was calibrated against the reaction: $ab = jd + qz$ at 29.5 kbar and 1,100° C (Holland 1980) and a −7% correction applied. Run times of 30–60 min were chosen as a compromise; shorter duration runs were very heterogeneous, but longer duration runs lost significant amounts of CO_2 (see below). Runs were quenched by turning off the power to the furnace; quench rates were 150–200° C/s. At the end of most runs, the buffer was examined and both phases found to be present. CO_2-free glasses of each composition were synthesized at high pressures by running both unwelded and welded silver oxalate-free inner capsules. Infrared spectra of these glasses did not differ from the infrared spectra of glasses of the same compositions prepared at 1 atm in air.

After quenching, the inner capsules were sectioned and doubly-polished plates of the bubble-free glasses were prepared. In most samples disseminated Ag metal gave the glass in the bottom of the capsule an orange color or blueish-orange streaked appearance. The thickness of each glass plate was measured using a micrometer

Table 1. Analyses of glass compositions used. Microprobe techniques are described within the text

Starting batch	jd ideal	jd-D	jd-E	jd-X	ab ideal	ab-E	ab-X	eu ideal	eu-E	eu-X
Na_2O	15.33	14.52	13.81	12.66	11.82	11.28	10.80	9.62	9.80	9.25
Al_2O_3	25.22	25.47	24.85	24.80	19.44	19.34	19.28	15.83	15.07	15.93
SiO_2	59.45	60.10	61.43	62.42	68.74	69.66	69.81	74.55	74.80	75.46
Total	100.00	100.09	100.09	99.88	100.00	100.38	99.89	100.00	99.67	100.64
# of analyses		12	4	6		7	7		6	3

Table 2. Comparison of wt. % CO_2 loaded into Pt capsules containing albite glass with total carbon (reported as wt. % CO_2) content of the quenched glass analyzed using the $^{12}C(d,p_0)^{13}C$ nuclear reaction. Run conditions were: 1.4 MeV deuterons, 15 nA beam current, 0.5 mm beam diameter, and 10 min irradiation times. Hilton calcite, from San Diego Co., Calif. was used as a standard, weighted by $(dE/dX)^{-1}$. Sensitivity at sample depths from 1 to 4 microns, eliminating surface contamination, and a detection limit of 100 ppm is estimated (Livi et al. 1984; Fine et al. 1985)

Sample #	CO_2 loaded (wt. %)	CO_2 analyzed (wt. %)
ABC-53	0.67	0.69
ABC-54	0.38	0.32
ABC-55	0.20	0.19
ABC-58	0.40	0.36

or dial indicator. The plates were placed over metal apertures 150–1,000 microns in diameter and their transmission infrared spectra were obtained. Spectra were gathered on a Perkin-Elmer 180 infrared spectrophotometer in the linear absorbance mode over the frequency range 4,000 cm^{-1} to 1,200 cm^{-1}. The sample chamber was purged with high purity N_2 while each spectrum was recorded. Spectra were recorded on chart paper and digitized with a Tektronix 4052 computer. The spectra of anhydrous, decarbonated glasses of each composition were then computer subtracted from these spectra. Both absorption intensities and integrated absorption intensities were determined from the background-subtracted digital data. The precision of absorbance data obtained in our laboratory is estimated to be about 0.01 (1σ) at an absorbance of 0.5 (Stolper 1982a).

Many of the glasses synthesized early in this study were not suitable for caliberation of absorption band intensities versus species concentration because they either were synthesized from melts held at pressure and temperature for less than 60 min or the final step in the drying procedure was not performed and the glasses were dark, presumably containing either graphite or a hydrocarbon residue. In the latter case, total dissolved carbon contents were presumed not to be accurately known. The infrared spectra of these glasses were still taken and data obtained from these samples, discussed below, were still useful.

After infrared spectra were taken, some of our albite glasses were independently analyzed for total carbon using the $^{12}C(d, p_0)^{13}C$ nuclear reaction. This technique, used by Filleux et al. (1977), Oberheuser et al. (1983), and Mathez et al. (1984), is discussed more fully in Livi et al. (1984) and Fine et al. (1985). It allowed us to independently determine the total C contents (within 5% relative certainty) of the same pieces of glass on which spectra were taken. These analyses show that after 1 h long runs, the amount of C analyzed after the run was within 10% of the amount loaded into the capsule (Table 2).

A few glasses were prepared using starting materials consisting of CO_2-free glass and Na_2CO_3 enriched with 90% ^{13}C as a CO_2 source rather than $Ag_2C_2O_4$. These glasses were enriched in Na and compositionally not on the $NaAlO_2$-SiO_2 join. CO_2-bearing *ab* and *jd* glasses prepared in the laboratory of Professor A. Boettcher were also used in the study. They were prepared using Na_2CO_3 or $Ag_2C_2O_4$ as CO_2 sources and were run at a variety of pressures and temperatures.

Experimental results

Band assignments

The spectra of a CO_2-free and a CO_2-bearing jadeite glass are shown in Figure 2. Four strong absorption bands are present in the CO_2-bearing glass at frequencies of higher

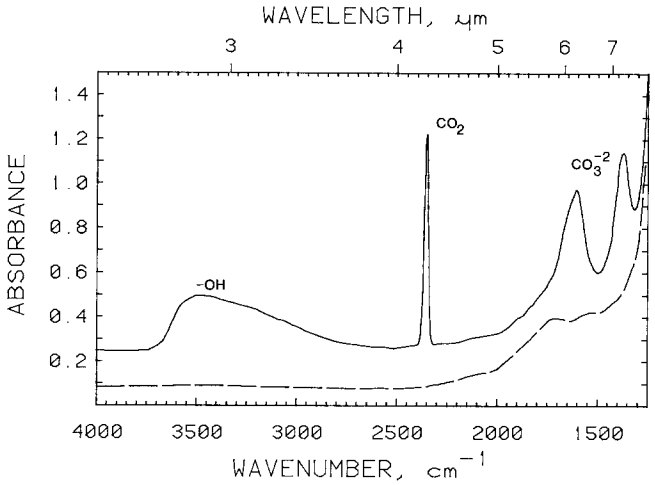

Fig. 2. Infrared spectrum (solid line) of a jadeite glass (JDC-84) containing 0.80 wt. % total dissolved CO_2 as measured by infrared spectroscopy. Band assignments are given. The dashed line is the spectrum of a CO_2-free jadeite glass synthesized at 1 atm. The silicate background has not been subtracted from either spectrum, hence the spectra go offscale at approximately 1,200 cm^{-1} due to aluminosilicate vibrations

than 1,200 cm^{-1} that are not present in the CO_2-free glass. Although their relative intensities vary with CO_2 content and glass composition (Figs. 3, 4, and 5 and Table 3) the locations of these four bands are essentially identical in all of the CO_2-bearing $NaAlO_2$-SiO_2 glasses that we have examined. At wavenumbers lower than 1,200 cm^{-1}, the vibrations of the aluminosilicate networks comprising these glasses result in absorption bands that go offscale.

The broad band at approximately 3,550 cm^{-1} is due to the stretching of —OH groups (Stolper 1982a) and was used to quantitatively measure the amount of H_2O dissolved in each glass using a molar absorptivity of 80 liters/mole-cm. Water contents of the CO_2-bearing glasses quenched from melts at high pressure typically range from 0.2 wt. % to 0.5 wt. % H_2O. We believe these levels of dissolved water to be unavoidable in experiments of this type, independent of drying procedure or the use of a double-capsule, buffered assembly. Water concentrations are higher in CO_2-bearing glasses than in those without CO_2. This suggests that adsorbed H_2O on the silver oxalate and/or hydrogen that diffuses through both the buffer and Pt capsule wall and reacts with CO_2 to produce H_2O and reduced carbon species during the experiments ware responsible for most of the water in these nominally anhydrous runs. Absorptions due to dissolved hydrocarbons or CO were not observed in any of our spectra. If reduced carbon is produced by reaction of hydrogen and dissolved CO_2 in our experiments, it is either not detectable via infrared spectroscopy (e.g., graphite) or diffuses out of our capsules (Watson et al. 1982). Preliminary experiments conducted in our laboratory and in the laboratory of Professor Boettcher have indicated that run lenghts of 3 or more hours result in significant depletions in spectroscopically measured total dissolved CO_2. If substantial carbon is lost or substantial reduced carbon is produced in shorter runs, it could modify some of the conclusions presented here. However, graphite is not observed in most of our run products and we have tried to minimize both the hydration of the glasses and

Table 3. Data obtained during this study

Sample	#	Starting comp.	P (kbar)	T (°C)	Duration (min)	CO_2 loaded (wt.%)	H_2O [a] (wt.%)	Density [b] (g/l)	Thickness (cm)	Band location	Abs.[h]	Integr.[i] Abs.	Band location	Abs.[h]	Integr.[i] Abs.	Band location	Abs.[h]	Integr.[i] Abs.
NC	2	eu-E	25	1450	30	1.81[c]	0.37	2440	0.0055	2350	1.80	67.96	1657	0.09	11.17	1379	0.11	6.60
NC	3	eu-E	25	1450	60	1.35[c]	0.41	2440	0.0043	2353	0.11	4.19	1650	0.01	1.44	1424	0.02	2.41
NC	4	eu-E	25	1450	60	0.45[c]	0.29	2440	0.0058	2353	0.88	24.84	1656	0.04	4.02	1358	0.04	4.42
NC	6	eu-E	25	1450	60	0.90[c]	0.42	2440	0.0063	2355	0.96	35.03	1650	0.07	8.26	1361	0.08	7.55
NC	7	eu-E	25	1450	60	0.60[c]	0.26	2440	0.0067	2352	1.06	30.92	1660	0.05	5.00	1407	0.07	7.00
NC	10	eu-E	25	1450	67	1.25[c]	0.39	2440	0.0043	2353	1.30	38.01	1652	0.06	6.93	1370	0.05	5.06
NC	13	eu-X	25	1450	60	0.00	0.14	2440	0.0167	2354	0.19	4.11	[d]			[d]		
NC	15	eu-X	25	1450	60	0.55	0.24	2440	0.0074	2354	1.33	38.18	[d]			[d]		
NC	17	eu-X	25	1450	60	0.25	0.18	2440	0.0083	2353	1.08	29.58	[d]			[d]		
NC	19	eu-X	25	1450	60	0.43	0.27	2440	0.0044	2355	1.04	27.79	[d]			[d]		
NC	20	eu-X	25	1450	60	0.20	0.38	2440	0.0073	2354	0.85	22.28	[d]			[d]		
NC	21	eu-X	25	1450	60	0.36	0.39	2440	0.0075	2353	1.46	38.92	[d]			[d]		
ABC	14	ab-E	25	1450	30	[c]	0.10	2530	0.0200	2355	0.03	0.14	[d]			[d]		
ABC	22	ab-E	25	1450	60	0.65[c]	0.21	2530	0.0060	2356	1.38	44.70	1620	0.14	17.98	1383	0.16	10.90
ABC	23	ab-E	33	1450	60	1.83[c]	0.65	2530	0.0026	2354	1.29	37.18	1614	0.16	21.22	1372	0.16	11.57
ABC	24	ab-E	33	1450	60	0.52[c]	0.22	2530	0.0056	2355	0.72	21.18	1620	0.09	11.70	1372	0.12	8.58
ABC	25	ab-E	33	1450	60	1.03[c]	0.39	2530	0.0037	2355	1.17	36.34	1618	0.15	20.13	1377	0.17	11.27
ABC	27	ab-E	27	1450	60	0.64[c]	0.39	2530	0.0046	2353	0.41	10.63	1619	0.05	6.16	1373	0.05	3.83
ABC	29	ab-E	15	1450	60	1.02[c]	0.86	2530	0.0030	2354	0.38	8.72	1606	0.05	5.30	1377	0.03	1.80
ABC	30	ab-E	15	1450	60	0.78[c]	0.49	2530	0.0036	2352	0.41	11.17	1611	0.04	4.15	1382	0.05	4.13
ABC	33	ab-E	25	1560	30	0.65[c]	0.27	2530	0.0046	2354	0.78	21.97	1618	0.06	7.54	1374	0.09	6.92
ABC	35	ab-E	25	1560	30	0.44[c]	0.21	2530	0.0067	2354	0.83	23.17	1622	0.07	8.59	1376	0.13	11.41
ABC	53	ab-E	25	1450	60	0.67	0.14	2530	0.0045	2353	1.43	36.60	1625	0.07	9.29	1374	0.13	10.36
ABC	54	ab-X	20	1450	60	0.38	0.16	2510	0.0055	2353	0.75	18.91	1626	0.04	4.42	1377	0.07	5.27
ABC	55	ab-X	20	1450	60	0.20	0.16	2510	0.0081	2353	0.48	11.63	1622	0.02	2.41	1380	0.10	9.62
ABC	56	ab-X	20	1450	60	0.49	0.30	2510	0.0051	2356	1.06	28.33	1619	0.04	3.87	1378	0.06	5.28
ABC	57	ab-X	20	1450	60	0.97	0.29	2510	0.0040	2354	0.97	25.21	1663	0.06	7.85	1384	0.09	6.87
ABC	58	ab-X	20	1450	60	0.40	0.18	2510	0.0070	2352	1.07	28.46	1610	0.06	8.94	1374	0.09	6.83
ABC	62	ab-X	20	1450	60	0.94	0.35	2510	0.0036	2353	1.37	36.49	1606	0.08	10.50	1375	0.10	6.51
ABC	64	ab-X	20	1450	60	0.75	0.15	2510	0.0058	2352	1.85	49.55	1616	0.13	19.18	1379	0.17	11.22
JDC	67	jd-D	25	1400	30	0.99[c]	0.26	2600	0.0053	2353	0.76	19.52	1605	0.24	27.92	1377	0.27	20.05
JDC	68	jd-D	25	1400	30	0.58[c]	0.39	2600	0.0073	2353	0.57	13.56	1605	0.29	30.00	1378	0.32	22.54
JDC	69	jd-D	25	1400	30	1.64[c]	0.42	2600	0.0033	2353	0.86	20.92	1607	0.32	35.38	1375	0.35	24.39
JDC	72	jd-D	25	1400	30	0.33[c]	0.37	2600	0.0080	2353	0.44	9.61	1604	0.21	21.68	1378	0.24	16.60
JDC	73	jd-D	25	1400	30	0.26[c]	0.50	2600	0.0062	2352	0.34	8.10	1603	0.21	21.22	1388	0.24	17.40
JDC	74	jd-D	25	1400	30	0.13[c]	0.60	2600	0.0071	2353	0.26	7.16	1606	0.15	16.35	1384	0.19	14.36
JDC	76	jd-D	25	1400	30	0.00[c]	0.65	2600	0.0049	2352	0.23	4.66	1643	0.05	4.83	1397	0.12	7.83
JDC	84	jd-D	25	1450	30	1.56[c]	0.35	2600	0.0044	2352	0.71	19.64	1611	0.30	33.56	1380	0.31	23.28
JDC	85	jd-D	25	1450	30	0.34[c]	0.24	2600	0.0089	2352	0.31	10.13	1612	0.18	18.95	1378	0.17	11.54
JDC	86	jd-D	25	1450	30	1.11[c]	0.30	2600	0.0055	2353	0.79	22.07	1610	0.36	38.19	1382	0.38	26.28
JDC	89	jd-D	25	1450	30	0.72[c]	0.32	2600	0.0027	2355	0.38	10.64	1612	0.18	21.49	1376	0.18	13.87
JDC	90	jd-D	25	1450	30	1.21[c]	0.33	2600	0.0052	2353	0.66	16.76	1613	0.28	31.42	1381	0.26	20.26
JDC	91	jd-D	25	1450	30	0.12[c]	0.30	2600	0.0041	2348	0.05	1.80	1625	0.04	5.05	1378	0.04	2.70
JDC	103	jd-X	25	1450	60	0.33	0.28	2600	0.0066	2353	0.65	17.62	1623	0.08	8.57	1383	0.05	2.79
JDC	108	jd-E	25	1450	60	0.96	0.13	2600	0.0041	2354	0.98	24.81	1609	0.33	37.52	1374	0.39	27.99
JDC	110	jd-E	25	1450	60	0.00	0.11	2600	0.0104	[d]			[d]			[d]		
JDC	111	jd-E	25	1450	60	0.17	0.12	2600	0.0115	2354	0.34	9.16	1607	0.16	19.44	1378	0.17	10.45
JDC	112	jd-E	25	1450	60	0.54	0.14	2600	0.0139	2354	1.23	36.61	1603	0.60	69.58	1380	0.64	43.98
JDC	113	jd-E	25	1450	60	0.39	0.18	2600	0.0059	2353	0.51	12.90	1617	0.19	21.71	1372	0.19	12.94
JDC	114	jd-E	25	1450	60	0.66	0.16	2600	0.0072	2354	0.46	11.47	1622	0.20	25.60	1371	0.25	18.58
JDC	116	jd-E	25	1450	60	0.56	0.12	2600	0.0109	2353	1.17	33.11	1607	0.54	61.82	1380	0.60	42.42
BOET2582[g]		jd	20	1450	15	SAT.[e]	0.43	2600	0.0018	2354	0.63	14.05	1595	0.33	36.05	1379	0.32	20.95
BOET2990[g]		ab	20	1450	360	1.00[f]	0.49	2510	0.0053	2354	1.12	28.76	1631	0.08	12.57	1363	0.09	6.42
BOET2995[g]		ab	20	1450	60	1.00	0.20	2510	0.0032	2355	1.22	35.21	1612	0.08	10.61	1369	0.09	6.11

[a] H_2O contents determined using the method of Stolper (1982a) and an extinction coefficient of 80 liters/mol-cm
[b] Densities either obtained or extrapolated from Kushiro (1978)
[c] Glasses were dark, presumably containing graphite and other reduced carbon species, so that total CO_2 contents are unknown
[d] Band intensity too low to characterize
[e] Vapor saturated, Na_2CO_2 used as a CO_2 source rather than $Ag_2C_2O_4$
[f] Total loaded CO_2 content believed unknown due to long run length (see text)
[g] Samples provided by Professor A. Boettcher
[h] Absorbance
[i] Integrated absorbance (cm^{-1})

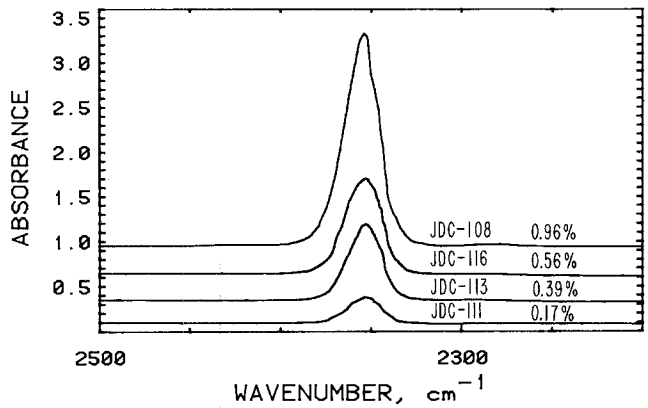

Fig. 3. Background subtracted spectra, from 2,500–2,200 cm^{-1} and all normalized to 100 microns sample thickness, of four jadeite composition glasses containing variable amounts of total dissolved CO_2. Sample numbers and total dissolved CO_2 contents are shown. The band at 2,352 cm^{-1} increases in a regular fashion with increasing total dissolved CO_2

obvious depletions of the glasses in spectroscopically observable carbon by run lengths of only 1 h. We emphasize that despite the most rigorous precautions, water seems to be unavoidable in these piston-cylinder experiments. In fact, water contents seem to be largely independent of our drying procedures and even the experiments conducted by Professor Boettcher utilizing special precautions to ensure dry conditions (Boettcher et al. 1981) contain dissolved water. Even C-free runs contain water. Our only consolation is that we are able to precisely measure water concentrations.

The sharp band at 2,352 cm^{-1} is attributed to the ν_3 antisymmetric stretch of molecular CO_2 (Mysen et al. 1975; Mysen et al. 1976; Mysen 1976; Brey 1976). We believe for several reasons that this molecular CO_2 is homogeneously dissolved at molecular scale, probably as weakly bond units located in holes or cages in the overall glass structure, rather than present as trapped fluid inclusions: The intensity of this band increases in a regular fashion with increasing total CO_2 content (Fig. 3). Our glasses are bubble-free when viewed at high power (500×) with an optical microscope and their total dissolved CO_2 contents are much lower than published CO_2 solubilities (Mysen 1976). Finally, the location of the band is slightly shifted from that of gaseous CO_2 at 2,349 cm^{-1} (Nakamoto 1978). When bubbled glasses are intentionally prepared and run, a double band suggestive of both gaseous CO_2 in bubbles and dissolved CO_2 is observed. Other arguments suggesting structurally bound CO_2, including SEM observations, are presented by Mysen et al. (1976).

The ν_3 antisymmetric stretch of a free, undistorted carbonate group (D_{3h} symmetry) results in a degenerate absorption band at ~1,415 cm^{-1}. Distortion of the CO_3^{2-} group (to C_{2v} on C_s symmetry) results in a loss of the degeneracy and the appearance of two bands (White 1974; Nakamoto 1978). Following Brey and Green (1975), we attribute the broad bands at 1,610 cm^{-1} and 1,375 cm^{-1} to the ν_3 stretch of distorted carbonate groups. Sharma (1979), Sharma et al. (1979a), and Mysen and Virgo (1980a) assigned analogous bands in other glass compositions the same way.

The constancy of the splitting of the ν_3 mode (~235 cm^{-1}) of carbonate ions in the glasses that we have studied suggests that the local environment of the carbonate group does not vary much over the range of Na_2O, Al_2O_3, SiO_2, and CO_2 contents of the glasses that we have studied. The degree of splitting we observe is much larger than that generally caused by symmetry lowering in crystalline carbonates (White 1974), but Nakamoto (1978) notes that either a unidentate (C_s) or bidentate (C_{2v}) carbonate complex (a carbonate ion coordinated to a metal atom) could have approximately the required splitting. The details of the observed splitting presumably provides important information on the local environment of CO_3^{2-} ions in the glasses, but we are unable to completely decipher these details at this time. Nevertheless, the large splitting that we observe is consistent with previous suggestions that carbonate ions are coordinated with sodium atoms in sodium aluminosilicate glasses (Mysen and Virgo 1980b). That the local carbonate environment is almost certainly dependent upon, if not dominated by, the charge-balancing or network modifying cations of the melt (Holloway et al. 1976) is confirmed by the fact that the ν_3 bands of CO_3^{2-} groups in a wide range of CO_2-bearing glasses with dominantly divalent network modifying cations, including basaltic glasses, glasses in the system CaO-Al_2O_3-SiO_2, and diopside and akermanite glasses (Rai et al. 1983; Sharma 1979; Sharma et al. 1979a; Fine and Stolper 1985) are split almost identically, but quite differently from the Na-bearing aluminosilicate glasses that we have studied.

Although we suggest that carbonate is present in our glasses as distorted sodium carbonate ionic-complexes, aluminium may also play an important role in the local environment of carbonate groups. This is suggested by the fact that the ν_3 carbonate bands of Al-poor Na_2O-Al_2O_3-SiO_2 glasses, and of Na_2O-SiO_2 glasses that we have examined (unpublished results) are, as in crystalline Na_2CO_3, not split to the extent observed in this study, if at all. The precise nature of the interaction between aluminium and sodium in the distortion of carbonate in our glasses cannot be addressed with our results and will require study of a wider range of silicate compositions on the Na_2O-Al_2O_3-SiO_2-CO_2 join.

There are other interpretations of the bands at 1,610 cm^{-1} and 1,375 cm^{-1} found in the literature. Often, the high energy bands has either not been recognized or not assigned to any C-bearing species (Mysen et al. 1975; Mysen 1976; Mysen et al. 1976). Mysen (1976) and Mysen et al. (1976) also suggest that in some instances, these bands may be due to HCO_3^-. Rai et al. (1983) conclude that the analogous doublet in CO_2-bearing diopside glass is due to two distinct carbonate sites in the glass. None of these suggestions can be readily reconciled with our observations that although the intensities of both bands increase with increasing total dissolved CO_2 (Fig. 4), their intensities are approximately equal to each other (1.17 $absorbance_{1610} = absorbance_{1375}$) regardless of total dissolved CO_2 content, silicate composition, or total dissolved H_2O (Fig. 6). We also note that the doublets in the diopsidic glasses of Rai et al. (1983), in the akermanite glasses of Sharma et al. (1979), and in basaltic glasses and glasses in the system CaO-Al_2O_3-SiO_2-CO_2 (Fine and Stolper 1985) mimic to within a few wavenumbers the splitting observed in the infrared spectrum of distorted CO_3^{2-} groups in scapolite. Scapolite contains only a single carbonate site (Papike and Stephenson 1966), rather than two carbonate sites or HCO_3^- groups.

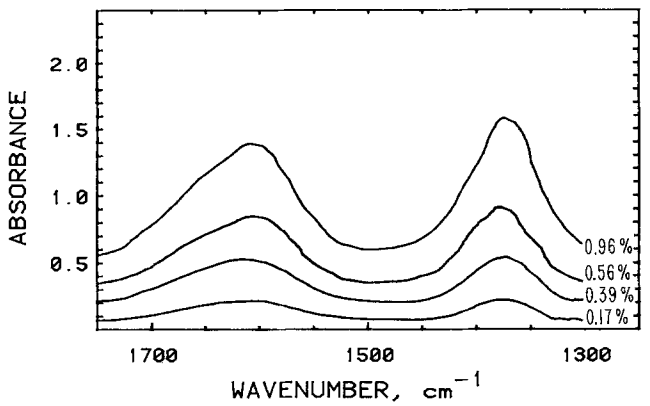

Fig. 4. Background subtracted spectra, from 1,800–1,200 cm^{-1} and normalized to sample thicknesses of 100 microns, of the same jadeite glasses shown in Fig. 3. Sample numbers and total dissolved CO_2 contents are shown. The bands at both 1,610 and 1,375 cm^{-1} increase with increasing total dissolved CO_2, yet their intensities are always approximately equal (1.17 $absorbance_{1610}$ = $absorbance_{1375}$)

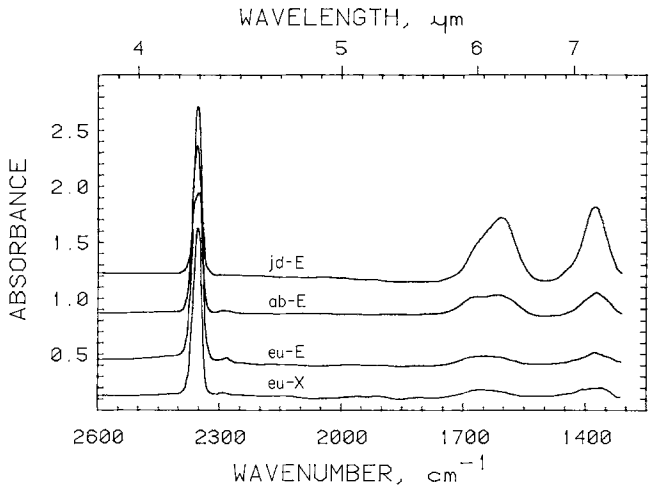

Fig. 5. Background subtracted spectra, from 2,600 to 1,200 cm^{-1}, of CO_2-bearing silicate glasses of four different compositions, *jd-E, ab-E, eu-E,* and *eu-X*. All of the spectra are normalized to constant intensity of the 2,352 cm^{-1} band. The intensities of the carbonate absorption bands increase with increasing Na content and decreasing silica content. (Samples shown are NC-10, NC-19, ABC-53, and JDC-108.)

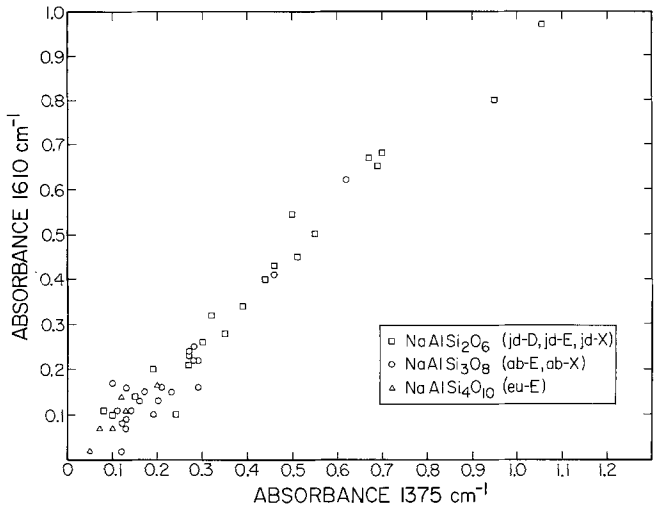

Fig. 6. Intensity of the carbonate absorption band at 1,375 cm^{-1} versus the intensity of the carbonate absorption band at 1,610 cm^{-1}, both normalized to 100 micron sample thickness, for all of the samples studied. The silicate composition of each glass is indicated. The intensities of both bands are approximately equal (1.17 $absorbance_{1610}$ = $absorbance_{1375}$) regardless of silicate composition, total CO_2 concentration, dissolved H_2O content, or the pressure and temperature from which the glass was quenched

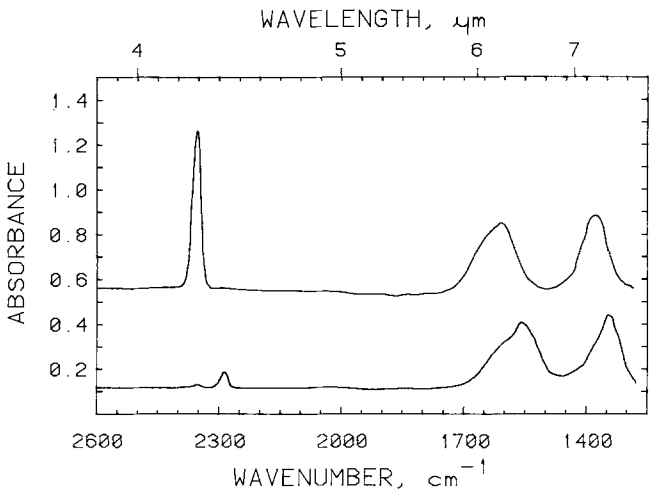

Fig. 7. Spectra of ^{12}C- (*top*) and 90% ^{13}C- (*bottom*) enriched jadeite glasses. The lowered ratio of the intensities of the molecular CO_2 bands to the intensities of the carbonate bands in the ^{13}C enriched glass are due to the additional Na_2O added to the glass

Table 3 presents the quantitative results obtained during this study, including the run conditions of all syntheses, the exact locations, intensities and integrated intensities of all of the aforementioned absorption bands, and the thickness and density of each sample studied.

Three other bands of low intensity were also observed during the course of this study. The band at 1,610 cm^{-1} is distorted due to the presence of an unassigned, broad, low intensity absorption band centered at ~1,680 cm^{-1}. Another band, at approximately 3,700 cm^{-1}, appears preliminarily to vary directly with the intensity of the 2,352 cm^{-1} band. It may be a combination of the ν_1 (Raman active only) + ν_3 modes of molecular CO_2. The intensity of a small band at 2,286 cm^{-1} also varies directly with the intensity of the 2,352 cm^{-1} band. We assign this band to the ν_3 antisymmetric stretch of molecular $^{13}CO_2$. Both of these bands are potentially useful for the determination of molecular CO_2 concentrations in glasses enriched in this component.

All of the band assignments attributed to C-bearing species are consistent with the spectra of $^{13}CO_2$-enriched glasses (Fig. 7). The band at 2,352 cm^{-1} is offset to 2,286 cm^{-1} as expected (Nakamoto 1978, p. 116), and the bands at 1,610 cm^{-1} and 1,375 cm^{-1} are lowered in frequency 50 cm^{-1} and 35 cm^{-1} respectively. The unidentified band at 1,680 cm^{-1} is also offset ~50 cm^{-1}, indicating that it too is due to a C-bearing species.

Calibration of band intensities versus species concentration

The Beer-Lambert law expresses the relationship between absorption band intensity and the concentration of either

Table 4. Calculated molar absorptivities and integrated molar absorptivities for infrared absorption bands due to C-bearing species

Band (cm^{-1})	Assignment	Molar absorptivity[a] (liters/mole-cm)	Integrated molar absorptivity[a] (liters/mole-cm^2)
2,352	molecular CO_2	945 ± 45	$25{,}200 \pm 1{,}200$
1,610	CO_3^{2-}	200 ± 15[b]	$24{,}100 \pm 1{,}900$
1,375	CO_3^{2-}	235 ± 20[b]	$16{,}800 \pm 1{,}500$

[a] Errors in these reported values were calculated assuming uncertainties of $\pm 10\%$ total loaded CO_2, of $\pm 2\%$ estimated density, of ± 0.02 absorbance units, and of ± 3 microns sample thickness. To the extent that reduced carbon species are present in these glasses or that the experiments lost carbon, the molar absorptivities have been underestimated

[b] These values are revised from the values of 300–400 liters/mole-cm presented in a preliminary report (Fine and Stolper 1984) due to improved background subtraction of our spectral data

CO_2 or CO_3^{2-}:

$$c = \frac{44.01 \times \text{absorbance}}{d \times \rho} \times \frac{1}{\varepsilon} \quad (1)$$

where c is the weight fraction of either CO_2 or CO_3^{2-} (expressed as a weight fraction of CO_2), 44.01 is the molecular weight of CO_2 in g/mole, absorbance is expressed in absorbance units, d is the sample thickness in cm, ρ is the sample density in g/liter, and ε is the molar absorptivity (or extinction coefficient) in liters/mole-cm. If integrated absorbances are measured instead of absorbances, the integrated molar absorptivity is substituted for molar absorptivity in Eq. (1). The total amount of carbon dissolved in a glass as molecular carbon dioxide and carbonate can be readily determined via infrared spectroscopy using Eq. (1) provided that the molar absorptivities of the band due to molecular CO_2 and one of the carbonate bands are known.

Molar absorptivities (and integrated molar absorptivities) for the 2,352 cm^{-1}, 1,610 cm^{-1}, and 1,375 cm^{-1} bands are listed in Table 4 and were determined by the following procedure: An equation was written giving total dissolved CO_2 as the sum of dissolved molecular CO_2, based on the absorbance of the 2,352 cm^{-1} band, and of CO_2 dissolved as carbonate, based on the absorbance of the 1,610 cm^{-1} band, for each of the 20 glasses for which total CO_2 contents were believed to be accurately known (see Table 3). The molar absorptivities of the 2,352 cm^{-1} and 1,610 cm^{-1} bands were then determined based on these 20 equations using a least squares method similar to that given by Albarede and Provost (1977) by which errors could be assigned to all of the parameters given in Equation (1) and to the best fit molar absorptivities. Three glasses (NC-15, ABC-57, and JDC-114) were anomalous, probably due to either errors in sample weighing or CO_2 loss during synthesis, and were ultimately rejected from the fitting procedure. The best fit value of the ratio of the extinction coefficients of the 1,610 cm^{-1} and 1,375 cm^{-1} bands was determined from the data shown in Figure 6 and the molar absorptivity of the 1,375 cm^{-1} band given in Table 4 is based on this ratio. The ratios of the integrated absorbances to absorbances for each of these bands were also determined by least squares and the integrated molar absorptivities listed in Table 4 are based on these ratios.

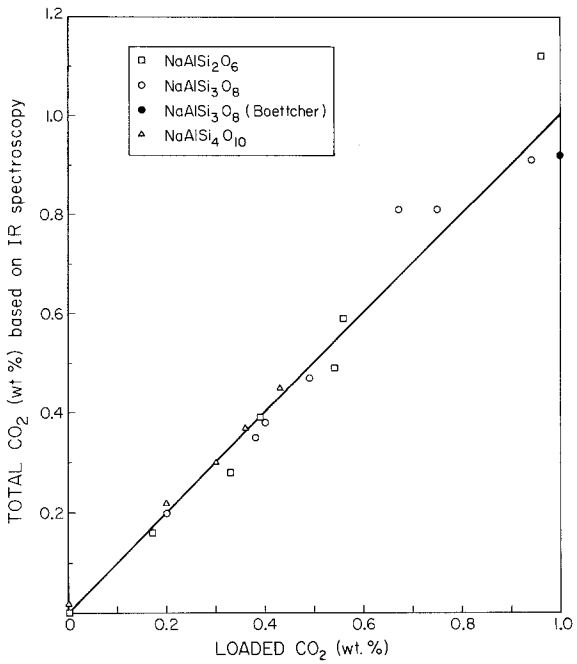

Fig. 8. Comparison of total CO_2 contents based on amount of silver oxalate loaded into the capsule and based on summing spectroscopically determined molecular CO_2 and CO_3^{2-} concentrations using the bands at 2,352 cm^{-1} and 1,375 cm^{-1}. Molar absorptivities are from Table 4. A line of loaded CO_2 = measured CO_2 is shown for reference. Samples shown are those used to determine molar absorptivities by least squares; the close correspondence of the data to a 45° line reflects the internal consistency of our calibration procedure. (Samples shown are NC-13, 17, 19, 20, 21; ABC-53, 54, 55, 56, 58, 62, 64; JDC-103, 108, 110, 111, 112, 113, 116, and BOET-2295)

Our procedure for determining molar absorptivities is based on two critical assumptions. First, molar absorptivities are assumed to be constant over the range of compositions studied and second, all dissolved CO_2 is assumed to be present as either molecular CO_2 or carbonate. The internal consistency of these assumptions can be tested by comparing total CO_2 concentrations, obtained by summing spectroscopically determined molecular CO_2 and carbonate concentrations, with the amounts of CO_2 originally loaded into the capsules. Figure 8 shows that the spectroscopically determined values adequately reproduce the total amount of CO_2 originally added to these glasses over the range of silicate compositions studied.

Infrared spectroscopy thus appears to be a useful tool for the measurement of CO_2 concentrations in glasses along the $NaAlO_2$-SiO_2 join to low levels of total dissolved carbon. Estimated detection limits are 25 ppm molecular CO_2 and 75 ppm CO_3^{2-} for a 200 micron thick piece of glass. Thicker samples would, from Eq. (1), have lower detection limits, but absorption bands due to aluminosilicate vibrations would tend to overwhelm the bands at both 1,610 cm^{-1} and 1,375 cm^{-1} in thicker specimens. Precision of relative CO_2 and CO_3^{2-} concentration measurements is estimated to be on the order of several percent based on uncertainties in absorbance, density, and sample thickness measurements. As reflected by the scatter to the data in Fig. 8, accuracy is estimated to be ± 15–20% at this time. As noted above, we think that uncertainties in loaded CO_2

Table 5. Concentrations (in wt.%) of molecular CO_2, CO_3^{2-}, and total CO_2 based on spectroscopic measurements. CO_3^{2-} concentrations are given as wt.% CO_2 dissolved as CO_3^{2-} and are based on the intensity of the 1,375 cm^{-1} band. The mole fractions of molecular CO_2 and CO_3^{2-} are also given. Mole fractions are computed on the basis of moles of assumed mixing species (i.e. CO_2, CO_3^{2-}, and O)

Sample	#	P (kbar)	T (°C)	CO_2 (mol.)	CO_3^{2-}	CO_2 (Tot.)	X_{CO_2}	$X_{CO_3^{2-}}$
NC	2	25	1450	0.62	0.15	0.78	0.0046	0.0011
NC	3	25	1450	0.05	0.04	0.08	0.0004	0.0003
NC	4	25	1450	0.29	0.05	0.34	0.0021	0.0004
NC	6	25	1450	0.29	0.10	0.39	0.0021	0.0007
NC	7	25	1450	0.30	0.08	0.38	0.0022	0.0006
NC	10	25	1450	0.58	0.09	0.67	0.0042	0.0007
NC	13	25	1450	0.02	0.00	0.02	0.0002	0.0000
NC	15	25	1450	0.34	0.00	0.34	0.0025	0.0000
NC	17	25	1450	0.25	0.00	0.25	0.0018	0.0000
NC	19	25	1450	0.45	0.00	0.45	0.0033	0.0000
NC	20	25	1450	0.22	0.00	0.22	0.0016	0.0000
NC	21	25	1450	0.37	0.00	0.37	0.0027	0.0000
ABC	14	25	1450	0.00	0.00	0.00	0.0000	0.0000
ABC	22	25	1450	0.42	0.20	0.62	0.0032	0.0015
ABC	23	33	1450	0.91	0.46	1.37	0.0068	0.0034
ABC	24	33	1450	0.24	0.16	0.40	0.0018	0.0012
ABC	25	33	1450	0.58	0.34	0.92	0.0043	0.0025
ABC	27	27	1450	0.16	0.08	0.24	0.0012	0.0006
ABC	29	15	1450	0.24	0.08	0.32	0.0018	0.0006
ABC	30	15	1450	0.22	0.11	0.32	0.0016	0.0008
ABC	33	25	1560	0.31	0.15	0.46	0.0023	0.0011
ABC	35	25	1560	0.23	0.14	0.37	0.0017	0.0011
ABC	53	25	1450	0.59	0.22	0.81	0.0044	0.0016
ABC	54	20	1450	0.25	0.10	0.35	0.0019	0.0007
ABC	55	20	1450	0.11	0.09	0.20	0.0008	0.0007
ABC	56	20	1450	0.39	0.09	0.47	0.0029	0.0006
ABC	57	20	1450	0.45	0.17	0.62	0.0034	0.0012
ABC	58	20	1450	0.28	0.10	0.38	0.0021	0.0007
ABC	62	20	1450	0.71	0.21	0.91	0.0053	0.0015
ABC	64	20	1450	0.59	0.22	0.81	0.0044	0.0016
JDC	67	25	1400	0.26	0.37	0.62	0.0020	0.0028
JDC	68	25	1400	0.14	0.32	0.46	0.0011	0.0024
JDC	69	25	1400	0.47	0.77	1.23	0.0036	0.0059
JDC	72	25	1400	0.10	0.22	0.32	0.0008	0.0017
JDC	73	25	1400	0.10	0.28	0.38	0.0008	0.0021
JDC	74	25	1400	0.07	0.19	0.26	0.0005	0.0015
JDC	76	25	1400	0.08	0.18	0.26	0.0006	0.0014
JDC	84	25	1450	0.29	0.51	0.80	0.0022	0.0039
JDC	85	25	1450	0.06	0.14	0.20	0.0005	0.0011
JDC	86	25	1450	0.26	0.50	0.76	0.0020	0.0038
JDC	89	25	1450	0.25	0.48	0.73	0.0019	0.0037
JDC	90	25	1450	0.23	0.36	0.59	0.0017	0.0028
JDC	91	25	1450	0.02	0.07	0.09	0.0002	0.0005
JDC	103	25	1450	0.18	0.05	0.23	0.0014	0.0004
JDC	108	25	1450	0.43	0.69	1.12	0.0033	0.0053
JDC	110	25	1450	0.00	0.00	0.00	0.0000	0.0000
JDC	111	25	1450	0.05	0.11	0.16	0.0004	0.0008
JDC	112	25	1450	0.16	0.33	0.49	0.0012	0.0026
JDC	113	25	1450	0.15	0.23	0.39	0.0012	0.0018
JDC	114	25	1450	0.11	0.25	0.37	0.0009	0.0019
JDC	116	25	1450	0.19	0.40	0.59	0.0015	0.0031
BOET	2582	20	1450	0.63	1.29	1.91	0.0048	0.0099
BOET	2990	20	1450	0.39	0.13	0.52	0.0029	0.0009
BOET	2995	20	1450	0.71	0.21	0.92	0.0053	0.0016

concentrations and problems with CO_2-loss during our experiments represent the major source of this scatter.

The extinction coefficients given in Table 4 have been used to obtain the amounts of molecular CO_2 and CO_3^{2-} dissolved in each of the glasses synthesized in this study. The results are presented in Table 5.

Speciation of carbon dioxide in silicate glasses

Figure 9 shows molecular CO_2 versus carbonate concentrations for *jd-E*, *ab-E*, and *eu-E* glasses synthesized at 1,450° C and 25 kbar with up to 1.1 wt.% total dissolved CO_2. For each silicate composition, the ratio of molecular

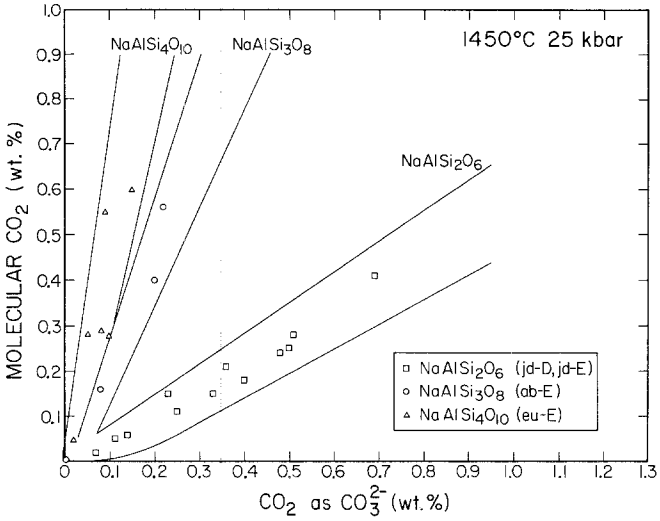

Fig. 9. Molecular CO_2 concentration versus the concentration of CO_2 dissolved as CO_3^{2-} for glasses on the $NaAlSi_2O_6$-SiO_2-CO_2 join quenched from melts held at 1,450° C and 25 kbar. Concentrations are spectroscopically determined. The trends defined by each composition as a function of total CO_2 content are outlined and reproduced in Figs. 10–12. (Data points are for NC-2, 3, 4, 6, 7, 10, ABC-14, 22, 27, 53, and JDC-84, 85, 86, 89, 90, 91, 108, 111, 112, 113, 114, 116)

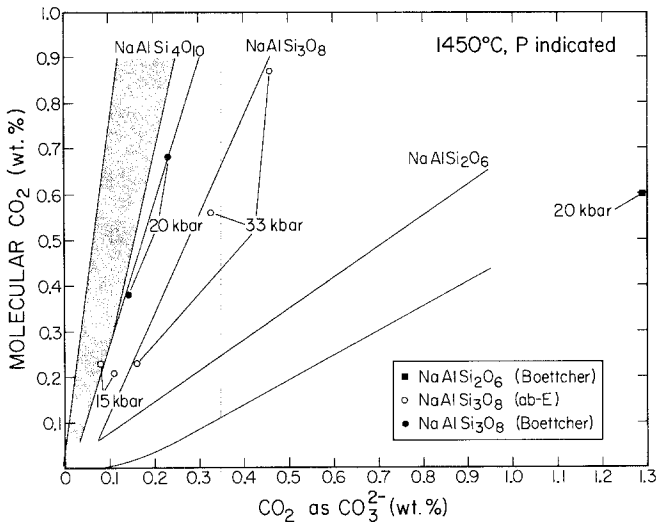

Fig. 10. Molecular CO_2 versus CO_2 dissolved as carbonate for glasses quenched from melts held at 1,450° C and pressures other than 25 kbar. The pressure of each run is marked. Trends are for glasses equilibrated at 1,450° C and 25 kbar (Fig. 9). Filled data points are from samples synthesized in the laboratory of A. Boettcher. (Data points are for ABC-23, 24, 25, 29, 30, and BOET 2582, 2990, 2995)

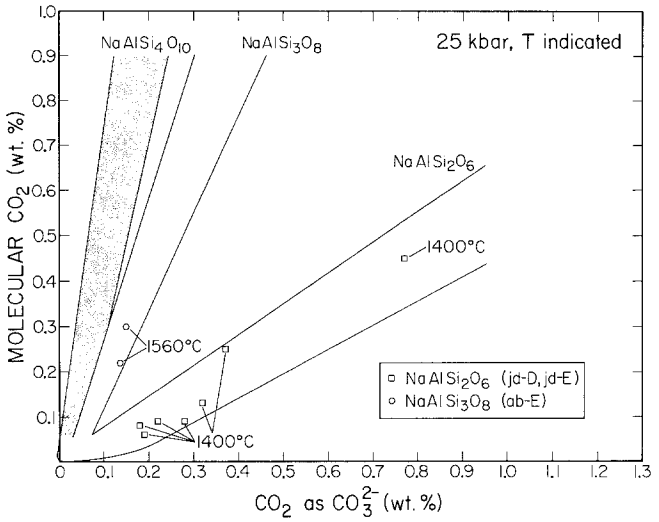

Fig. 11. Molecular CO_2 versus CO_2 dissolved as carbonate for glasses quenched from melts held at 25 kbar and temperatures other than 1,450° C. The temperature of each run is marked. Trends are for glasses equilibrated at 1,450° C and 25 kbar (Fig. 9). (Data points are for ABC-33, 35, and JDC-68, 69, 72, 73, 74, 76)

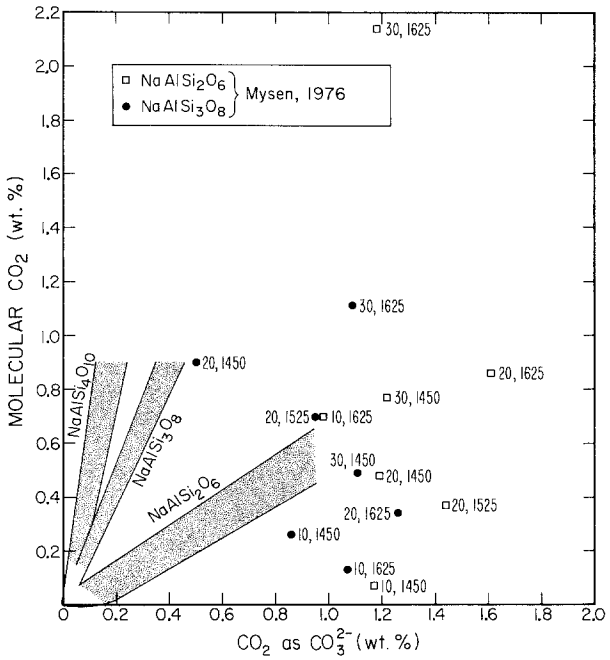

Fig. 12. Molecular CO_2 concentration versus the concentration of CO_2 dissolved as CO_3^{2-} for glasses on the $NaAlO_2$-SiO_2-CO_2 join comparing the data of Mysen (1976) with our results (*shaded regions*). Mysen's data points are labelled with the pressure and temperature of the melt prior to quenching. There is essentially no correlation between the two data sets

CO_2 to CO_3^{2-} dissolved in the glasses varies little over the range of total CO_2 contents studied. The ratio is, however, a strong function of silicate composition, increasing with increasing silica and decreasing soda and alumina content along the $NaAlO_2$-SiO_2 join. CO_2 dissolves in *jd* glass predominantly as CO_3^{2-}; the ratio of molecular CO_2 to CO_2 as CO_3^{2-} is approximately 0.6. In *ab* and *eu* glasses, molecular CO_2 predominates; the ratios are approximately 2.3 and 5, respectively. Glasses prepared from compositions that lost Na during the initial drying processes (*jd-X, ab-X, eu-X*) have higher, but still constant molecular CO_2 to CO_3^{2-} ratios. The ratio is 3.4 in *jd-X* glasses and 2.7 in *ab-X* glasses. *Eu-X* glasses contain negligible CO_3^{2-}.

We have also studied glasses of *ab-E, ab-X* and *jd-E* compositions quenched from melts held at pressures and temperatures other than 1,450° C and 25 kbar. While there is some variation suggesting a slight increase in the ratio of molecular CO_2 to carbonate with decreasing temperature

and pressure (Figs. 10–11), the variations are minor for each of the compositions we have studied. The pressure and temperature dependence that we have observed is small when compared to previously reported results (Mysen 1976 and Fig. 12). We conclude that the speciation of CO_2 in glasses on the $NaAlO_2$-SiO_2 join is not strongly dependent on pressure and temperature over the 15–33 kbar, 1,400–1,560° C ranges.

The ratios of molecular CO_2 to CO_3^{2-} of the *ab* and *jd* CO_2-bearing glasses synthesized in the laboratory of Professor A. Boettcher are similar to those of our CO_2-bearing *ab-E* and *jd-E* glasses (Fig. 10). Since these glasses were synthesized using both Na_2CO_3 and $Ag_2C_2O_4$ as CO_2 sources and were held at melt conditions for a variety of run lengths, we take this correspondence to be indicative of equilibrium between CO_2 species in the glasses we have studied.

Since none of our runs were anhydrous, it is difficult to assess the role of H_2O in the CO_2 speciation trends we observe. Previous workers (Eggler and Rosenhauer 1978) have stated that H_2O enhances the formation of CO_3^{2-}. We see no relationship between the ratio of molecular CO_2 to CO_3^{2-} and the H_2O contents of the samples that we have studied. However, the water contents of our glasses are low; higher water contents may well influence the speciation of CO_2.

Discussion

Comparison with previous spectroscopic investigations

Our results are comparable with those of Mysen (1976), who used infrared spectroscopy to investigate CO_2 dissolution in glasses quenched from vapor-saturated melts on the $NaAlO_2$-SiO_2-CO_2 join. Mysen et al. (1976) also reported infrared studies of CO_2-bearing $NaAlSi_3O_8$ glass. In addition, Brey (1976) studied CO_2-bearing glasses on the $NaAlSi_3O_8$-$CaAl_2Si_2O_8$ join with infrared spectroscopy, and Raman spectroscopy was used to investigate glasses in this system by Mysen and Virgo (1980b). In all of these studies, as in ours, glasses were synthesized by quenching from melts held at high pressures and temperatures in piston-cylinder apparatuses. The pressures and temperatures from which the melts were quenched were similar in all of these investigations. One difference between these previous studies and ours is that they focussed on saturated systems whereas most of the glasses that we examined were quenched from vapor-undersaturated melts.

There is little disagreement about the *existence* of both molecular CO_2 and carbonate in CO_2-bearing sodium aluminosilicate glasses, although Brey (1976) states, without supporting evidence, that the molecular CO_2 is a quenching phenomenon. We confirm the conclusion of Mysen (1976) that the speciation of CO_2 in silicate melts is strongly dependent on silicate composition, with the ratio of molecular CO_2 to carbonate increasing with increasing silica content on the $NaAlO_2$-SiO_2 join. There is, however, little quantitative correspondence between our measured molecular CO_2 and carbonate contents and those reported by Mysen (1976) (Fig. 12). We see no evidence of the strong pressure and temperature dependence of CO_2 speciation that Mysen (1976) reported. Finally, we find essentially constant carbonate to molecular CO_2 ratios for each silicate composition as total dissolved CO_2 content increases; Mysen and Virgo (1980b) reported that the CO_3^{2-} to molecular CO_2 ratio increases with total dissolved CO_2 in albite glasses.

Why are our results so different from those of Mysen (1976)? The total CO_2 contents of the glasses studied by Mysen tend to be at the high end of those studied by us, since his experiments were vapor-saturated while most of ours were not. The *P–T* conditions and total CO_2 contents of these two studies overlap, however, and the results should be comparable. We suspect the explanation of the discrepancies between results lies principally in differences in analytic techniques. Mysen (1976) used a mixture of $Ba^{14}CO_3$ and Na_2CO_3 as a CO_2 source and measured the total dissolved carbon content of each of his glasses by β-track counting. Then, using the intensity of the 7.2 micron ($\sim$1,375 cm^{-1} in this study) carbonate band, which he calibrated using mixtures of powdered CO_2-free silicate glass and Na_2CO_3 embedded in KBr discs, he determined the concentration of CO_3^{2-} dissolved in each glass. Molecular CO_2 concentrations were determined by the difference between the total carbon content and the CO_3^{2-} content.

One limitation of the procedure employed by Mysen (1976) is that uncertainties in bulk CO_2 content determined by β-track mapping and in carbonate concentration determined by infrared spectroscopy propagate into estimations of molecular CO_2 content. One potential problem is that all of the carbon detected by β-tracking may not be dissolved or present as oxidized species. Other possible uncertainties associated with the use of β-track mapping for bulk carbon analysis have been discussed by Brey (1976) and Rai et al. (1983).

There are also uncertainties associated with Mysen's (1976) determination of carbonate concentrations via infrared spectroscopy. Infrared spectra were obtained on discs of KBr in which powdered glasses were embedded. Numerous studies (Duyckaerts 1959; Tuddenham and Lyon 1970; Russell 1974; Wong and Angell 1976) have indicated that extreme care must be taken with KBr pellets and that quantitative results are difficult to obtain. Our experience has confirmed that KBr spectra are often quite difficult to interpret, especially in the case of these CO_2-bearing glasses, in which relevant band intensities are quite low. Particle size has a large effect on absorption spectra and care must be taken to reproducibly grind samples. Grinding can, in some cases, structurally alter the material of interest. Adsorption of gases on both the KBr and the ground sample may also be significant (Barker and Torkelson 1975). It is clear that many of the earlier studies that used infrared spectroscopy on KBr pellets to study volatile speciation in glasses suffered from these difficulties. Therefore, many of the conclusions drawn from them are suspect. In particular, the conclusions that molecular CO_2 is a detectable constituent of nearly all C-bearing glasses, including basic compositions such as diopside and several natural rock compositions (Mysen et al. 1975; Mysen et al. 1976), and that its concentration varies systematically with conditions of melt equilibration were almost certainly artifacts. In the case of diopside, molecular CO_2 has not been detected by Raman spectroscopy (Sharma 1979; Mysen and Virgo 1980a; Rai et al. 1983). We have studied one of the glasses synthesized by Rai et al. (1983) [Di #89] and conclude, using a molar absorptivity for the 2,352 cm^{-1} band of 945 liters/mole-cm, that the concentration of molecular CO_2 is less than 25 ppm by weight. We have also failed to detect any molecular CO_2 in synthetic CO_2-rich basaltic glasses

or in glasses in the system CaO-Al_2O_3-SiO_2-CO_2 (Fine and Stolper 1985). A combination of adsorbed CO_2 and incomplete purging of the sample chamber (Brey 1976) may have been responsible for the spurious molecular CO_2 observed in the spectra of Mysen et al. (1975, 1976). Examination of the spectra of Mysen et al. (1975), Mysen et al. (1976), and Mysen (1976) suggests that water adsorbed on the KBr was probably also a problem, resulting in major absorptions at $\sim 3{,}500$ and $\sim 1{,}600\ cm^{-1}$. Eggler et al. (1979) also suggest that adsorbed acetone can produce significant absorptions in spectra of powdered materials.

There may also be problems with the procedure used by Mysen (1976) to calibrate the intensity of the $\sim 1{,}375\ cm^{-1}$ carbonate band. The carbonate band is split by $\sim 200\ cm^{-1}$ in $NaAlO_2$-SiO_2 glasses and only slightly split in Na_2CO_3 (White 1974), suggesting that caution should be used in equating the integrated molar absorptivities for the carbonate groups in these two systems. Indeed, our measured integrated molar absorptivity for the $1{,}440\ cm^{-1}$ (actual location) band in Na_2CO_3 (determined using KBr pellets) is $\sim 36{,}500$ liters/mol-cm^2, more than twice the value we have obtained for the $1{,}375\ cm^{-1}$ band. We are also puzzled by the fact that Mysen's (1976) calibration curve for the $\sim 1{,}400\ cm^{-1}$ carbonate band (his Fig. 10) is not linear and does not pass through zero and that the area he measures to determine concentration is described in his text as "transmittance", whereas absorbance would be the usual measurement used for determining the CO_3^{2-} concentration.

By taking our spectra on doubly-polished glass plates, we have avoided the problems associated with KBr pellets. Most important, however, is the fact that we measure molecular CO_2 and carbonate band intensities simultaneously in each glass plate. Thus, even if our determinations of molar absorptivities are in error, leading to inaccuracies in the measured concentrations of the various species, the ratios of band intensities, and thus variations in the relative proportions of dissolved C-bearing species, can be precisely determined. This contrasts with the approach used by Mysen (1976) in which the concentration of molecular CO_2 was determined by difference between independent determinations of total dissolved CO_2 and carbonate concentrations. Using Mysen's approach, meaningful determinations of the relative proportions of molecular CO_2 and carbonate depend on both the accuracy and precision of the total CO_2 and carbonate concentrations. We believe that these factors explain the differences between the two data sets in Fig. 12.

One final potential advantage of our technique over the use of KBr pellets is that the infrared beam may be aimed at particular spots in the sample. Glasses may be checked for homogeneity or diffusion gradients and glass pockets interstitial to crystals can be analyzed. The size of the "spot" that can be analyzed will depend on the spectrometer and will be ultimately limited by diffraction, but spot sizes on the order of a few tens of microns or better are achievable with modern instrumentation.

Our results indicate that at relatively low concentrations of CO_2 in silicate glasses, the ratio of molecular CO_2 to carbonate in a glass varies little with total dissolved CO_2 content. Using Raman spectroscopy, Mysen and Virgo (1980b) found that over a similar range of pressure, temperature and CO_2 content, the ratio of carbonate to molecular CO_2 increased with increasing total CO_2 content for albite glasses. It is difficult to evaluate this conclusion since Mysen and Virgo (1980b) give no quantitative details. There is neither a demonstration of a linear variation in band intensity with species concentration, nor a discussion of the precision and accuracy of their determinations of band intensities, nor a consideration of their detection limits for CO_2 and CO_3^{2-} in glasses. The band at $\sim 1{,}075\ cm^{-1}$ that they use to infer CO_3^{2-} concentration is deeply buried among three silicate bands, and its intensity can only be determined by deconvolution procedures. This probably means that the detection limit and precision for CO_3^{2-} concentrations determined by this procedure are poor. Apparently confirming this, they saw no CO_3^{2-} in an albite glass containing 0.68 weight percent total CO_2, whereas in equivalent glasses that we have studied, carbonate is readily detected. It also appears from Fig. 3 of Mysen and Virgo (1980b) that the intensity of the band at $\sim 1{,}378\ cm^{-1}$ that they have assigned to molecular CO_2 increases roughly in proportion to their CO_3^{2-} band between 2.05 wt.% and 3.20 wt.% total CO_2. Their data might be consistent with a roughly constant molecular CO_2 to carbonate ratio. Thus, the apparent discrepancy between the Raman spectroscopic results of Mysen and Virgo (1980b) and our infrared results may simply reflect the fact that infrared spectroscopy is, at this stage, more useful as a tool for measuring the concentrations of C-bearing species in silicate glasses. A similar conclusion was reached by Stolper (1982a) regarding measurement of the concentrations of water and hydroxyl groups in glasses.

Speciation of CO_2 in silicate melts

Although our spectroscopic measurements are on CO_2-bearing *glasses* quenched from melts, our principal interest is in the behavior of CO_2-bearing melts. Throughout the remainder of this paper, we will assume that the speciation of CO_2 that we have measured in glasses accurately reflects that of the melts from which they were quenched. Support for this assumption comes from numerous comparisons between the properties of melts and glasses at 1 atm (e.g., Taylor et al. 1980; Seifert et al. 1981; Okuno and Marumo 1982; Aines et al. 1983) and from the fact that the speciation of water in glasses quenched from melts does not appear to be affected by quenching provided that quenching is done rapidly (Stolper et al. 1983).

Water, like carbon-dioxide, dissolves in silicate glasses and melts both in molecular form and as ions (hydroxyl in the case of water and carbonate in the case of carbon dioxide) produced by reaction between the molecular species and oxygen atoms of the silicate melt (Stolper 1982a). The homogeneous equilibrium between melt species has been described as follows for water-bearing melts:

$$H_2O\ (\text{molecular}) + O^{2-} = 2OH^- \tag{2}$$

with an equilibrium constant:

$$K_1 = \frac{(a^m_{OH^-})^2}{(a^m_{O^{2-}})\,(a^m_{H_2O,\,mol})} \tag{3}$$

where a^m refers to the activity of each of the melt species. At very low concentrations of dissolved water, the concentration of unreacted oxygen is essentially the same as in anhydrous melt, because it has not decreased either by dilution with molecular water or by extensive conversion to hydroxyl groups, and $a^m_{O^{2-}}$ can be treated as constant. The

activities of hydroxyl and molecular water can be approximated by their mole fractions (Stolper 1982b) and therefore:

$$\frac{(X^{m}_{OH})^2}{(X^{m}_{H_2O,\,mol})} \simeq (a^{m}_{O^{2-}})(K_1) \simeq \text{constant}. \quad (4)$$

Therefore, at low total water concentrations the concentration of molecular water in melts is expected to be proportional to the square of the concentration of hydroxyl groups. This is related to the oft-quoted "square-root" relationship between the fugacity of water in melts and its mole fraction at low total water contents (Stolper 1982b).

A similar treatment can be applied to the equilibrium between molecules of CO_2 and carbonate in melts. The homogeneous equilibrium between melt species can be described with the following sort of reaction:

$$CO_2\ (\text{molecular}) + O^{2-} = CO_3^{2-}, \quad (5)$$

with an equilibrium constant:

$$K = \frac{(a^{m}_{CO_3^{2-}})}{(a^{m}_{O^{2-}})\,(a^{m}_{CO_2,\,mol})}. \quad (6)$$

We can envision CO_2 solution as the mixing of CO_2 molecules with C-free silicate melt species. These react according to reaction (5), producing carbonate, until the equilibrium constant K is satisfied.

It is likely that not all oxygens in silicate melts are equally reactive with molecular CO_2 to produce carbonate. Thus, for each distinguishable type of oxygen in the melt, a reaction such as (5) can be written, each having its own value of K (Eq. 6). Many of the oxygen species in silicate melts may be effectively inert with respect to CO_2. K in Eq. (6) would be approximately zero for these oxygen species. For purposes of discussion, we will assume that one reaction of the form of Eq. (5) is dominant and thus that O^{2-} in Eq. (5) refers to a subset of the oxygens in the melt (e.g., to the bridging, non-bridging, or free oxygens in the sense of Toop and Sammis 1962). Thus $a^{m}_{O^{2-}}$ will be less than 1 for CO_2-free melts and will probably vary with the silicate composition of the melt.

The relationships between the activities of molecular CO_2, carbonate, various types of oxygen atoms in the melt, and melt composition are not obvious and are not likely to be simple. In this discussion, we envision the melt to be a mixture of CO_2 molecules, carbonate groups, and oxygen atoms, analogous to the model developed by Stolper (1982b) for molecular water, hydroxyl groups, and oxygen atoms in hydrous melts. In the latter case, an ideal mixture of these species was assumed, giving activities equal to mole fractions. In the case of a mixture of CO_2 molecules, carbonate groups, and oxygen atoms, the fact that the each species has a different size complicates the relationship between activity and composition even for ideal (in the sense that all configurations are energetically equivalent) mixtures. In these situations, volume fractions have greater significance than mole fractions (Flory 1944; 1953, Chapter XII; Guggenheim 1952, Chapter X). For the simple analysis given here, however, we will assume that activity equals mole fraction for each species, keeping in mind that this is only an approximation. Mole fraction in this context refers to the number of moles of a particular mixing species in the mixture over the total number of species. For example, for a melt consisting of 1 mole of CO_2 molecules, 3 moles of CO_3^{2-} groups, and 1 mole of $NaAlSi_2O_6$ (6 moles of O), $X_{CO_2,\,mol} = 0.1$ and $X_{CO_3^{2-}} = 0.3$.

If we consider only low total CO_2 contents, such that $a^{m}_{O^{2-}}$, the activity of the reactive oxygen species, can be treated as approximately constant and the activities of the carbon-bearing species can be approximated by their mole fractions, Eq. (6) can be approximated by:

$$\frac{(X^{m}_{CO_3^{2-}})}{(X^{m}_{CO_2,\,mol})} \simeq (a^{m}_{O^{2-}})\,(K) \simeq \text{constant}. \quad (7)$$

Our observation that for each composition there is an approximately linear relationship between the concentration of molecular CO_2 and carbonate up to $\sim 2\%$ total CO_2 (Figs. 9–11) is thus precisely what we would expect based on homogeneous equilibrium between melt species.

Although the CO_2/CO_3^{2-} ratio increases as silica increases along the $NaAlO_2$-SiO_2 join, it is not clear whether this should be attributed to decreasing soda and alumina or to increasing silica. Our experiments on silicate compositions that lost sodium during extended drying at 800° C (*ab-X, jd-X,* and *eu-X*) point to a major role for the sodium concentration. Even the relatively minor soda losses experienced by these compositions (resulting in slightly peraluminous bulk compositions) result in dramatic increases in the ratio of molecular CO_2 to carbonate in the glasses. Indeed, this is how we were first alerted that these compositions were depleted in soda.

The observed variations in speciation with melt composition can be readily rationalized in terms of Eqs. (6) and (7). Suppose that the equilibrium constant K in Eq. (6) does not vary over the range of compositions that we have studied. It is then clear from Eq. (7) that at low total dissolved CO_2 contents, the ratio of CO_3^{2-} to molecular CO_2 would increase with increasing soda content, provided that the basicity of the melt (i.e., the activity of reactive oxygens, $a^{m}_{O^{2-}}$) increases with increasing soda content. This would be the case, for example, if CO_2 molecules reacted primarily with non-bridging oxygens or free oxygens (Toop and Sammis 1962; Pearce 1964; Wagner 1975), since in both cases the concentrations of these oxygens are expected to be correlated with Na_2O content.

As it is written, reaction (5) does not explicitly take into account the changes in the speciation of the C-free aluminosilicate matrix of the melt that accompany formation of carbonate (e.g. changes in degree of polymerization, etc.) However, a linear relationship between $X^{m}_{CO_3^{2-}}$ and $X^{m}_{CO_2,\,mol}$ is expected to hold at low total CO_2 contents for each silicate composition regardless of the details of the reactions describing the molecular CO_2-carbonate-oxygen interactions. The linearity results from the fact that one carbon dioxide molecule is converted into one carbonate group and from the approximation that the activities of the oxygen species are constant. For example, a linear relationship would also be expected to hold at low CO_2 concentrations if reaction (5) were replaced by:

$$CO_2\ (\text{molecular}) + 2O^{-} = CO_3^{2-} + O^{\circ} \quad (8)$$

where O^{-} and O° refer to non-bridging and bridging oxygens, respectively, in the sense of Toop and Samis (1962). This is the kind of reaction proposed by Eggler and Rosenbauer (1978) for the production of carbonate groups in diopside and other basic melt compositions.

At high total dissolved CO_2 contents the relationship between the concentration of molecular CO_2 and carbonate

is expected to deviate from linearity when the approximations that $a_{O^{2-}}$ in Eq. (6) or that a_{O^-} and a_{O° in the equivalent expression for Eq. (8) are constant break down. Under these circumstances, we would expect that the molecular CO_2/carbonate ratio would begin to increase with increasing total CO_2, as in the case of the solution of water, where the ratio of molecular water to the square of the hydroxyl concentration eventually begins to increase as water content increases (Stolper 1982b). Just where the expected deviation from linearity would become noticeable is unclear, but it must be at >1% total CO_2 in the compositions that we have studied (Fig. 9). If a reaction such as that described in Eq. (8) describes the molecular level interactions between molecular CO_2 and carbonate in sodium aluminosilicate melts, the linear relationship could extend to relatively high total CO_2 contents. In such a case, the activity of the major species O° might be changed little by the addition of small amounts of carbonate and the activity of O^-, a minor species, might be buffered by interactions with other C-free melt species and change very little even after substantial molecular CO_2 has been converted to CO_3^{2-}. This will be true for any carbonate-producing reaction involving relatively minor oxygen species whose concentrations might be essentially buffered by the concentrations of major species not greatly affected by the addition of carbonate or molecular CO_2.

Spera and Bergman (1980) analyzed available data on the pressure and temperature dependence of CO_2 solubility in silicate melts using a thermodynamic model of CO_2-bearing silicate melts in which the activity of CO_2 dissolved in the melt was assumed to be proportional to the mole fraction of total dissolved CO_2. Our results also suggest that the relationship between activity and composition in CO_2-bearing melts can be approximated as linear. This follows from the fact that the activity of CO_2 in the melt can be assumed to be roughly equal or proportional to the mole fraction of dissolved *molecular* CO_2, which is in turn approximately proportional to total dissolved CO_2 because carbonate and molecular CO_2 contents are proportional. Our results can thus explain why Spera and Bergman's "ideal" model for the relationship between a_{CO_2} and the mole fraction of total dissolved CO_2 is so successful at explaining phase equilibrium data.

Spera and Bergman (1980) also used available solubility data to determine $\bar{V}_{CO_2}$, the partial molar volume of CO_2 in silicate melts, for a number of melts including albite, jadeite, and nepheline. Recall that most of the dissolved CO_2 in albite is molecular CO_2, whereas most in nepheline is expected to be carbonate. That Spera and Bergman (1980) found $\bar{V}_{CO_2}$ to be essentially identical for these melts despite the difference in their speciation suggests that the volume change accompanying reactions such as (5) and (8) are minor. This is consistent with our observation that CO_2 speciation is only weakly dependent on pressure.

Solubility of CO_2 in silicate melts

The equilibrium between silicate melt and CO_2-bearing vapor can be modelled by the following heterogeneous equilibrium:

$$CO_2^{vapor} = CO_2^{melt}\ (\text{molecular}) \tag{9}$$

with an equilibrium constant:

$$K_{CO_2} = \frac{a^m_{CO_2,\,mol}}{a^v_{CO_2}} = \frac{a^m_{CO_2,\,mol}}{f_{CO_2}/f^\circ_{CO_2}} \sim \frac{X^m_{CO_2,\,mol}}{f_{CO_2}/f^\circ_{CO_2}} \tag{10}$$

where $a^m_{CO_2,\,mol}$ and $a^v_{CO_2}$ refer to the activities of molecular CO_2 in the melt and CO_2 in the vapor. The fugacity of CO_2 in the vapor is f_{CO_2} and of CO_2 in pure CO_2 vapor is $f^\circ_{CO_2}$. The standard state for CO_2 in the vapor is pure CO_2 vapor at pressure and temperature; i.e., $a^v_{CO_2}$ is 1 at all pressures and temperatures for pure CO_2 vapor and less than one if the vapor contains other constituents. The standard state for molecular CO_2 in the melt is a fictive form of pure CO_2 at pressure and temperature such that the activity coefficient of molecular CO_2 in the melt approaches 1 as its concentration approaches zero. The reciprocal of K_{CO_2} can thus be regarded as a Henry's law constant and the approximation given in Eq. (7) ($a^m_{CO_2,\,mol} \sim X^m_{CO_2,\,mol}$) will be strictly true as long as Henry's law holds.

If K_{CO_2} is only weakly dependent on melt composition for melts near the $NaAlO_2$-SiO_2 join, this would mean that the mole fraction of molecular CO_2 ($X^m_{CO_2,\,mol}$) would be similar in all melts equilibrated with pure CO_2 vapor at a given pressure and temperature. The total CO_2 solubility is the sum of CO_2 dissolved as molecular CO_2 and carbonate; therefore since the amount of dissolved carbonate at constant $X^m_{CO_2,\,mol}$ increases from silicate to jadeite (Fig. 9), we would anticipate from our results that CO_2 solubility should also increase in this order. This is precisely what is observed (Mysen 1976). In our view, variations in the solubility of CO_2 in each of these water-poor melts as functions of pressure and temperature would be due mostly to variations in K_{CO_2} as a function of pressure and temperature, because CO_2 speciation is only weakly dependent on pressure and temperature.

It should be possible, given the measured solubility of CO_2 in one melt composition at a given pressure and temperature, to use our CO_2 speciation data to calculate the solubility of CO_2 in other melt compositions at the same pressure and temperature. Our speciation data suggest that the ratio of the solubility of total CO_2 in albite melts to that in jadeite melts should be ~0.54. Mysen (1976) reported that this ratio ranged from 0.65 at 1,625° C and 20 kbar to 0.90 at 1,450° C and 10 kbar. We consider the agreement to be satisfactory given the possible uncertainties in Mysen's measurements and our own absolute CO_2/CO_3^{2-} measurements. Our analysis also suggests that pure silica liquid would dissolve CO_2 essentially entirely as molecular CO_2; the solubility of CO_2 will then be ~70% of that in albite melt, assuming that at saturation $X^m_{CO_2,\,mol}$ is the same in all melts. Based on the data of Mysen (1976), this suggests a solubility of 1.2 wt.% CO_2 in metastable silica melt at 20 kbar, 1,625° C and 1.7 wt.% at 30 kbar, 1,625° C. The results of Boettcher (1984) on phase equilibria in the system SiO_2-CO_2-H_2O also suggest a nontrivial solubility of CO_2 in silica melts.

Solubility mechanisms of CO_2 in silicate melts

We regard silicate melts as dynamic, with the homogeneous equilibria between oxygen species continually readjusting as they are perturbed by the addition of CO_2 or other components. Thus, even if only a single kind of oxygen actually reacts with molecular CO_2 to form carbonate, the concentrations of other oxygen species will be affected as they act to buffer the single reactive oxygen species. Thus, even if the concentrations of the different oxygen species could be determined, it may be extremely difficult to specify which classes of oxygen are directly involved in carbonate-produc-

ing reactions and which are passively responding to these reactions. There has, however, been considerable speculation about the structural role played by the oxygens that react with CO_2 molecules to produce carbonate groups and about the structural changes that occur in the silicate framework of these melts when reactions such as (5) proceed.

It is widely believed, based on Raman spectra (Mysen and Virgo 1980b; Sharma et al. 1978, 1979b), X-ray scattering data (Taylor et al. 1979), and thermochemical studies (e.g. Navrotsky et al. 1982), that $NaAlO_2$-SiO_2 glasses and melts are nearly fully polymerized in the sense that every oxygen is shared between two silicate and/or aluminate tetrahedra. It is difficult to envision how CO_2 molecules can react with a melt in which there are only bridging oxygens to produce carbonate. One possibility is for the resulting carbonate ion to participate in the bridge between adjacent tetrahedra by forming silicon- or aluminium-bearing carbonate complexes (Sharma et al. 1979a). An example of such a structure might be:

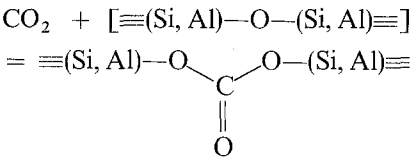

Carbonate concentration decreases as silica is added to melts, suggesting that oxygens bridging two Si tetrahedra do not react with CO_2 molecules in this way. However, we cannot rule of the formation of such structures between Al and Si tetrahedra or between two Al tetrahedra. In these cases, sodium atoms that provided charge-balance for the bridging oxygens prior to reaction with CO_2 molecules would probably be associated with the newly formed structure in some way. We have no data indicating if complexes like this are present in our glasses, but do note that these CO_3^{2-} groups would undoubtedly be highly asymmetric and that this unusual environment could, in principle, account for the splitting of the ν_3 carbonate band that we observe.

Another possibility is that bridging oxygens are removed from the silicate-aluminate network when they react with CO_2 molecules to produce carbonate ions. In such cases, structural and charge balance considerations are usually taken to require local rearrangements in the silicate and aluminate framework. For example, Mysen and Virgo (1980b) suggested that reaction of CO_2 molecules with bridging oxygens to produce carbonate groups is accompanied by the generation of octahedrally-coordinated aluminum. Other configurations, such as five-fold or three-fold coordination of aluminum (McKeown et al. 1984) or aluminum triclusters (Lacy 1963) could also be generated by such reactions. None of these reaction products has been positively identified by spectroscopy in CO_2-free or CO_2-bearing glasses, although their concentration may be expected to be quite high in very carbonate-rich aluminosilicate glasses. Mysen and Virgo (1980b) include weak bands they interpret as reflecting the presence of octahedrally-coordinated aluminum in their deconvolutions of the Raman spectra of CO_2-rich glasses.

We doubt that CO_2-free melts on the join $NaAlO_2$-SiO_2 are *fully* polymerized. The undoubtedly contain non-bridging and even free oxygens at some concentration level, probably some non-tetrahedrally coordinated aluminum (Boettcher et al. 1982, 1984), and perhaps aluminum triclusters. It may be that molecules of CO_2 react with two non-bridging oxygens to produce a bridging oxygen and a carbonate group in much the same way that carbonate groups are thought to be produced in depolymerized melts such as diopside (Eggler and Rosenhauer 1978). Alternatively, free oxygen could react with CO_2 to form carbonate complexes (Tomlinson 1953; Pearce 1964; Wagner 1975). Only small amounts of non-tetrahedrally coordinated aluminum or of aluminum triclusters would be required to produce enough non-bridging or free oxygens to account for the observed concentrations of CO_3^{2-} groups in the glasses we have studied. In addition, as reactive oxygens are consumed and carbonate ions are generated, the concentrations of the reactive oxygens might be regenerated to some extent by the equilibria between these and the major oxygen species; relatively large amounts of carbonate could be produced by reaction of CO_2 molecules with non-bridging or free oxygens even if the concentrations of these species in melts are small.

We emphasize that most of these and the equivalent statements of previous workers are highly speculative. Reliable and sensitive techniques for quantitatively determining both the concentrations of different types of oxygens and local configurations in glasses are needed before statements about changes in melt structure that accompany carbonate formation can be made with confidence.

Water versus CO_2 speciation

There are some important differences between the behavior of water and carbon dioxide in silicate melts that can be evaluated in light of the previous discussion of homogeneous equilibria in melts. In contrast to the case of carbon dioxide, the speciation of water in melts shows very little dependence on silicate composition. For example, variations in the proportions of molecular water and hydroxyl groups between melts on the $NaAlSi_2$-SiO_2 join or between these and melts on the $CaAlSi_2O_8$-SiO_2 join appear to be minor (L.A. Silver and E. Stolper, unpublished results) whereas CO_2 speciation varies dramatically over this composition range. Likewise, total water solubility is only weakly dependent on silicate composition, whereas carbon dioxide solubility is strongly dependent on melt composition (Eggler and Rosenhauer 1978).

Mono- and divalent cations probably play roles in the solubility mechanisms of water in the silicate melts in which they are present. However, these roles appear to be minor compared to those that they play in the case of CO_2 solubility, where such cations seem to be essential for the formation of carbonate groups and where energetic differences between different metal-carbonate complexes may dominate both the speciation and solubility behavior of CO_3^{2-} in melts. In other words, all of the oxygens in silicate melts can be regarded as nearly equally available for reaction with water molecules via Eq. (2). Although the OH groups formed by such a reaction may be associated with the Na, Ca, etc. in melts that contain such cations, these metal hydroxide complexes seem to be energetically similar. The result is that variations in K_1 in Eq. (4), which is an expression of the variation in the free energy differences between these species in the melt, are minor and K_1 values of 0.1–0.3 seem to satisfy most hydrous systems. In contrast, it seems likely that only certain types of oxygens are available for

reaction with CO_2 molecules in Eq. (5). Thus, even if K in Eq. (6) is constant for a series of melts, the carbonate to molecular CO_2 ratio can vary from melt to melt due to variations in the activity of the reactive oxygen species ($a^m_{O^{2-}}$ in Eq. (6)). In addition, the energetics of the reaction (i.e., the stability of the carbonate complex relative to the left hand side of Eq. (5)) may depend dramatically on the cations present in the melt; that is, K for reaction (5) may be strongly dependent on the mono- and divalent cations that are present and perhaps on other compositional factors. The strong composition dependence of CO_2 speciation and solubility in melts may thus be viewed as a combination of the variations in concentrations of "reactive" oxygen species (i.a., $a^m_{O^{2-}}$ in Eq. (6)) and of the equilibrium constants of the homogeneous equilibria governing the interactions between CO_2 and CO_3^{2-} (i.e., K in Eq. (6)) with melt composition.

Conclusions

1. Infrared spectroscopy can be used to quantitatively determine the concentrations of molecular CO_2 and carbonate groups in silicate glasses. If doubly-polished glass plates are used instead of powders embedded in KBr pellets, species concentrations can be measured with a precision on the order of several percent of the amount present. This technique has the potential for analyzing individual spots with diameters on the order of 10 μm. The absolute accuracy of species concentrations measurements is currently limited to about ±15–20% in the glasses that we have studied, but this can be improved with suitable standards.

2. Glasses in the system Na_2O-Al_2O_3-SiO_2-CO_2 near the $NaAlSi_2O_6$-SiO_2-CO_2 join that have been quenched from melts at 15–33 kbar, 1,400–1,560° C contain both carbonate and CO_2 molecules. Carbonate groups are in distorted environments very different from those in crystalline carbonates. The carbonate groups may be in the form of Na-carbonate ion-complexes.

3. There is an approximately linear relationship between molecular CO_2 and carbonate concentrations for each of the silicate compositions we have studied, up to at least 1% total dissolved CO_2. The molecular CO_2 to carbonate ratio is strongly dependent on the silicate composition of the glass, with the proportion of molecular CO_2 increasing as silica is approached on the $NaAlSi_2O_6$-SiO_2 join. Compositions that differ only in their soda concentrations have different molecular CO_2 to carbonate ratios, with those that have lower Na_2O contents having higher ratios. The strong dependence of CO_2 speciation on glass compositions contrasts with the situation for the speciation of water in glasses.

4. The speciation of CO_2 in glasses quenched from melts is only weakly dependent on the pressure or temperature at which the melt was equilibrated over the 15–33 kbar, 1,400–1,560° C range. This is similar to results for water speciation, but contrasts with previously reported results for CO_2.

5. We propose that the speciation of CO_2 in silicate melts in controlled by homogeneous equilibria between CO_2 molecules, carbonate groups, and oxygen atoms in the melts. The approximately linear relationship between molecular CO_2 and carbonate concentrations can be readily understood by considering the thermodynamics of such equilibria. The strong dependence of the molecular CO_2 to carbonate ratio can also be accounted for if the melt is considered to contain several different oxygen species, only some of which react with molecular CO_2 to produce carbonate. The observed compositional dependence is consistent with the hypothesis that soda concentration is the major factor controlling the availability of oxygens for reaction with molecular CO_2 to form carbonate and that the carbonate is dissolved as sodium carbonate complexes.

6. Observed variations in total CO_2 solubility with melt composition can be understood using our measured species concentrations and simple thermodynamic considerations. The approximately linear relationship between the activity of CO_2 in melts and the mole fraction of total dissolved CO_2 that has been proposed by Spera and Bergman (1980) can also be readily understood using our results.

7. Our results demonstrate that infrared spectroscopic measurements of species concentrations in glasses provide a direct approach to developing a quantitative understanding of the molecular level interactions involved in the solubility of CO_2 in silicate melts and of the thermodynamic properties and phase equilibria of CO_2-bearing silicate melts.

Acknowledgments. The spectroscopic measurements used in this study were performed in the laboratory of Professor George Rossman at Caltech. The guidance of Professor Rossman and the help of Roger Aines, Stephanie Mattson, and Martin Ruzek is gratefully acknowledged. Professor A. Boettcher, R. Luth and Dr. S. Sharma provided samples. S. Epstein performed C analyses. Professors D. Burnett and T. Tombrello, and Drs. M. Mendenhall and R. Livi, all of Caltech, made analysis of C using nuclear reaction techniques possible. P. Ihinger provided invaluable laboratory assistance. Reviews by Art Boettcher, John Holloway, Björn Mysen and one anonymous reviewer are appreciated. Supported by NSF grant EAR-8212765. Caltech Division of Geological and Planetary Sciences Contribution Number 4147.

References

Aines RD, Silver LA, Rossman GR, Stolper E, Holloway JR (1983) Direct observation of water speciation in rhyolite at temperatures up to 850° C. Geol Soc Am Abstr with Prog 15:512

Albarede F, Provost A (1977) Petrological and geochemical mass-balance equations: an algorithm for least-squares fitting and general error analysis. Comp Geosci 3:309–326

Barker C, Torkelson BE (1975) Gas adsorption on crushed quartz and basalt. Geochim Cosmochim Acta 39:212–218

Boettcher AL (1984) The system SiO_2-H_2O-CO_2: melting, solubility mechanisms of carbon, and liquid structure to high pressures. Am Mineral 69:823–833

Boettcher AL, Windom KE, Bohlen SR, Luth RW (1981) Low friction, anhydrous, low- to high-temperature furnace sample assembly for piston-cylinder apparatus. Rev Sci Instrum 52:1903–1904

Boettcher AL, Burnham C. Wayne, Windom KE, Bohlen SR (1982) Liquids, glasses, and the melting of silicates to high pressures. J Geol 90:127–138

Boettcher AL, Guo Q, Bohlen S, Hanson B (1984) Melting in feldspar-bearing systems to high pressures and the structures of aluminosilicate liquids. Geol 12:202–204

Brey G (1976) CO_2 solubility and solubility mechanisms in silicate melts at high pressures. Contrib Mineral Petrol 57:215–221

Brey G, Green DH (1975) The role of CO_2 in the genesis of olivine melilitite. Contrib Mineral Petrol 49:93–103

Brey G, Green DH (1976) Solubility of CO_2 in olivine melilitite at high pressures and the role of CO_2 in the earth's upper mantle. Contrib Mineral Petrol 55:217–230

Duyckaerts G (1959) The infrared analysis of solid substances – a review. Analyst 84:201–214

Eggler DH (1973) Role of CO_2 in melting processes in the mantle. Carnegie Inst Washington Yearb 72:457–467

Eggler DH (1974) Effect of CO_2 on the melting of peridotite. Carnegie Inst Washington Yearb 73:215–224

Eggler DH (1978) The effect of CO_2 upon partial melting of peridotite in the system Na_2O-CaO-Al_2O_3-MgO-SiO_2-CO_2 to 35 kb, with an analysis of melting in a periodite-H_2O-CO_2 system. Am J Sci 278:305–343

Eggler DH, Rosenhauer M (1978) Carbon dioxide in silicate melts: II. Solubilities of CO_2 and H_2O in $CaMgSi_2O_6$ (diopside) liquids and vapors at pressures to 40 kb. Am J Sci 278:64–94

Eggler DH, Mysen BO, Hoering TC, Holloway JR (1979) The solubility of carbon monoxide in silicate melts at high pressures and its effect on silicate phase relations. Earth Planet Sci Lett 43:321–330

Fine G, Stolper E (1984) Infrared spectroscopy of carbon dioxide-bearing silicate glasses. Geol Soc Am Abstr with Prog 16:508

Fine G, Stolper E (1985) Carbon dioxide in basaltic glasses: concentrations and speciation. Earth Planet Sci Lett (submitted)

Fine G, Stolper E, Mendenhall MH, Livi RP, Tombrello TA (1985) Measurement of the carbon content of silicate glasses using the $^{12}C(d,p_0)^{13}C$ nuclear reaction. In: Armstrong JT (ed) Microbeam Analysis – 1985. San Francisco Press, pp 241–245

Filleux C, Tombrello TA, Burnett DS (1977) Direct measurement of surface carbon concentrations. Proc Lunar Sci Conf 8th, pp 3755–3772

Flory PJ (1944) Thermodynamics of heterogeneous polymers and their solutions. J Chem Phys 12:425–438

Flory PJ (1953) *Principles of polymer chemistry*. Cornell University Press

Guggenheim EA (1952) *Mixtures*. Oxford University Press

Holland TB (1980) The reaction albite = jadeite + quartz determined experimentally in the range 600–1,200° C. Am Mineral 65:129–134

Holloway JR, Mysen BO, Eggler DH (1976) The solubility of CO_2 in liquids on the join CaO-MgO-SiO_2-CO_2. Carnegie Inst Washington Yearb 75:626–630

Kushiro I (1975) On the nature of silicate melt and its significance in magma genesis: regularities in the shift of the liquidus boundaries involving olivine, pyroxene, and silica minerals. Am J Sci 275:411–431

Kushiro I (1978) Viscosity and structural changes of albite ($NaAlSi_3O_8$) melt at high pressures. Earth Planet Sci Lett 41:87–90

Lacy ED (1963) Aluminum in glasses and in melts. Phys Chem Glasses 4:234–238

Livi RP, Mendenhall MH, Tombrello TA, Fine G, Stolper E (1984) High sensitivity carbon content analyses of geological materials using 1.4 MeV deterons. Proc Int Symposium on Nuclear Accelerator Physics (Laboratori Nazional di Legarno, Italy) (in press)

Mathez EA, Blacic JD, Berry J, Maggiore C, Hollander M (1984) Carbon abundances in mantle minerals determined by nuclear reaction analysis. Geophys Res Lett 11:947–950

McKeown DA, Waychunas GA, Brown GE (1984) Na and Al environments in some minerals and a series of glasses within the Na_2O-Al_2O_3-SiO_2 system. Geol Soc Am Abstr with Prog 16:589

Mysen BO (1976) The role of volatiles in silicate melts: solubility of carbon dioxide and water in feldspar, pyroxene and feldspathoid melts to 30 kb and 1,625° C. Am J Sci 276:969–996

Mysen BO, Virgo D (1980a) Solubility mechanisms of carbon dioxide in silicate melts: a Raman spectroscopic study. Am Mineral 65:885–899

Mysen BO, Virgo D (1980b) The solubility behavior of CO_2 in melts on the join $NaAlSi_3O_8$-$CaAl_2Si_2O_8$-CO_2 at high pressures and temperatures: a Raman spectroscopic study. Am Mineral 65:1166–1175

Mysen BO, Arculus RJ, Eggler DH (1975) Solubility of CO_2 in natural nephelinite, tholeite and andesite melts to 30 kb pressure. Contrib Mineral Petrol 53:227–239

Mysen BO, Eggler DH, Seitz MG, Holloway JR (1976) Carbon dioxide in silicate melts and crystals: Part I. Solubility measurements. Am J Sci 276:455–479

Nakamoto K (1978) *Infrared and Raman spectra of inorganic and coordination compounds* (3rd edn). John Wiley and Sons

Navrotsky A, Peraudeau G, McMillan P, Coutures JP (1982) A thermochemical study of glasses and crystals along the joins silica-calcium aluminate and silica-sodium aluminate. Geochim Cosmochim Acta 46:2039–2047

Oberheuser G, Kathrein H, Demortier G, Gonska H, Freund F (1983) Carbon in olivine single crystals analyzed by the $^{12}C(d,p)^{13}C$ method and by photoelectron spectroscopy. Geochim Cosmochim Acta 47:1117–1129

Okuno M, Marumo F (1982) The structures of albite and anorthite melts. Mineral J Japan 11:180–196

Papike JJ, Stephenson NC (1966) The crystal structure of mizzonite, a calcium- and carbonate-rich scapolite. Am Mineral 51:1014–1027

Pearce ML (1964) Solubility of carbon dioxide and variation of oxygen ion activity in soda-silica melts. J Am Ceramic Soc 47:342–347

Rai CS, Sharma SK, Muenow DW, Matson DW, Byers CD (1983) Temperature dependence of CO_2 solubility in high pressure quenched glasses of diopside composition. Geochim Cosmochim 47:953–958

Russell JD (1974) Instrumentation and techniques. In: VC Farmer (ed) *The infrared spectra of minerals*. Mineral Soc London Mon 4:11–25

Seifert FA, Mysen BO, Virgo D (1981) Structural similarity of glasses and melts relevant to petrological processes. Geochim Cosmochim Acta 45:1879–1884

Sharma SK (1979) Structure and solubility of carbon dioxide in silicate glasses of diopside and sodium melilite compositions at high pressures from Raman spectroscopic data. Carnegie Inst Washington Yearb 78:532–537

Sharma SK, Virgo D, Mysen BO (1978) Structure of melts along the join SiO_2-$NaAlSiO_4$ by Raman spectroscopy. Carnegie Inst Washington Yearb 77:652–658

Sharma SK, Hoering TC, Yoder HS (1979a) Quenched melts of akermanite composition with and without CO_2 – Characterization by Raman spectroscopy and gas chromatography. Carnegie Inst Washington Yearb 78:537–542

Sharma SK, Virgo D, Mysen BO (1979b) Raman study of the coordination of aluminum in jadeite melts as a function of pressure. Am Mineral 64:779–787

Spera FJ, Bergman SC (1980) Carbon dioxide in igneous petrogenesis: I. Aspects of the dissolution of CO_2 in silicate liquids. Contrib Mineral Petrol 74:55–66

Stolper E (1982a) Water in silicate glasses: An infrared spectroscopic study. Contrib Mineral Petrol 81:1–17

Stolper E (1982b) The speciation of water in silicate melts. Geochim Cosmochim Acta 46:2609–2620

Stolper E, Silver LA, Aines RD (1983) The effects of quenching rate and temperature on the speciation of water in silicate glasses. EOS, Trans Am Geophys Union 64:339

Taylor M, Brown GE, Jr, Fenn PM (1980) Structure of mineral glasses – III. $NaAlSi_3O_8$ supercooled liquid at 805° C and the effects of thermal history. Geochim Cosmochim Acta 44:109–117

Tomlinson JW (1953) Some aspects of the constitution of liquid oxides. In: *Physical chemistry of melts*. London Inst Min Metall pp 22–33

Toop GW, Samis CS (1962) Activities of ions in silicate melts. Trans Met Soc AIME 224:878–887

Tuddenham WM, Lyon RJP (1960) Infrared techniques in the iden-

tification and measurement of minerals. Anal Chem 32:1630–1634
Verweij H, Van den Boom H, Breemer RE (1977) Raman scattering of carbonate ions dissolved in potassium silicate glasses. J Am Ceram Soc 60:529–534
Wagner C (1975) The concept of basicity of slags. Met Trans 6B:405–409
Watson EB, Sneeringer MA, Ross A (1982) Diffusion of dissolved carbonate in magmas: Experimental results and applications. Earth Planet Sci Lett 61:346–358
White WB (1974) The carbonate minerals. In: WC Farmer (ed) *The infrared spectra of minerals*. Mineral Soc London Mon 4:227–284
Wong J, Angell CA (1976) *Glass structure by spectroscopy*. Marcel Dekker, Inc
Wyllie PJ (1979) Magmas and volatile components. Am Mineral 64:469–500

Received October 22, 1984 / Accepted May 21, 1985